REVIEW

Check for updates

A review on recent progress in polymer composites for effective electromagnetic interference shielding properties – structures, process, and sustainability approaches

Rajesh Kumar Bheema,[a] Gopu J, [iD][a] Krithika Bhaskaran,[a] Akshat Verma,[a] Murthy Chavali [iD][b] and Krishna Chaitanya Etika [iD] *[a]

The rapid proliferation and extensive use of electronic devices have resulted in a meteoric increase in electromagnetic interference (EMI), which causes electronic devices to malfunction. The quest for the best shielding material to overcome EMI is boundless. This pursuit has taken different directions, right from materials to structures to process, up to the concept of sustainable materials. The emergence of polymer composites has substituted metal and metal alloy-based EMI shielding materials due to their unique features such as light weight, excellent corrosion resistance, and superior electrical, dielectric, thermal, mechanical, and magnetic properties that are beneficial for suppressing the EMI. Therefore, polymer nanocomposites are an extensively explored EMI shielding materials strategy. This review focuses on recent research developments with a major emphasis on structural aspects and processing for enhancing the EMI shielding effectiveness of polymer nanocomposites with their underlying mechanisms and some glimpses of the sustainability approaches taken in this field.

1 Introduction

Electronic communications technology has significantly improved over the years, and a variety of electrical devices are now widely employed in several sectors such as communications, civic, aircraft, military, and others.[1] Furthermore, these electronic devices emit electromagnetic (EM) waves continuously during operation, resulting in electromagnetic interference (EMI) between electrical appliances that has a detrimental impact on the operational accuracy of electronic equipment in the electronics industry.[2] However, EMI has become a new form of pollution due to the proliferation of electronic devices in the past few decades. The effects of this EMI can cause service interruption, data loss, permanent damage to equipment, and failure.[3] Owing to such issues, the researchers investigated several methods for preparing EMI shielding materials in the quest for the perfect shielding material.

Metals are excellent conductors of electricity and may reflect EM waves; hence, metals are widely used in EMI shielding applications.[4–7] However, the shielding mechanism in metals is dominated by the reflection of EM waves, which is not always a desirable option.[4,5] In addition, relatively large densities and high production costs limit their extensive EMI shielding applicability.[8,9] Due to these limitations of metals researchers focused on using polymers for EMI shielding applications because of their properties such as light weight, flexibility, low density, ease of processing, chemical and thermal stability, and most importantly, scalability. The polymers mostly allow the EMI waves to pass through the surface for absorption phenomena to happen rather than reflection, which occurs in metals.[10] Polymer nanocomposites (PNC) represent a class of materials that possess a unique combination of electrical, thermal, dielectric, magnetic, and/or mechanical properties.[4–7,11] PNC characteristics may be tailored for EM wave suppression depending on the type of polymer and filler utilized. Due to their appealing properties, polymer nanocomposites have been considered an alternative to metals for EMI shielding applications.[4,5,12]

Furthermore, polymer-based composites containing lossy dielectric materials and/or magnetic materials are used to eliminate EMI and protect electronic devices from unwanted EM waves through absorption and reflection. In general, absorption dominant shielding materials are preferable for equipment over reflection, because reflection can cause additional interference to nearby equipment.[13] To mitigate these problems caused by signal interference, efficient shielding materials are required to defend the normal operation of electronic systems. Furthermore, EMI shielding materials should have desirable characteristics such as low density, large

[a]*Department of Chemical Engineering, BITS Pilani, Pilani, Rajasthan 333 031, India. E-mail: etika.krishna@pilani.bits-pilani.ac.in*

[b]*Office of the Dean Research, Dr. Vishwanath Karad MIT World Peace University, Survey No, 124, Paud Rd, Kothrud, Pune, Maharashtra 411038, India*

absorption capability, thin, light weight, and wide-range frequency bandwidth.[14] In addition, the selection of materials will also play an important role in designing EMI shielding materials. Recent studies have demonstrated the growing demand for low-cost and efficient EMI shielding materials as a consequence of the greater usage of electronic devices and electrical systems in industrial applications in the microwave frequency range.[15–18] Furthermore, several studies on thin, lighter weight, effective shielding materials suitable for large bandwidth absorption have been reported.[19–23] Furthermore, effective polymeric EMI shielding materials containing carbon-based fillers and metal-based fillers, and conducting polymers have been reported in the literature.[4–7,11,24,25] However, poor dispersion, phase separation, and high filler content are the main challenges in these studies. Owing to such limitations, various structural and processing strategies have been developed to achieve efficient EMI shielding materials.[26–30] This paper provides a comprehensive overview of structural and processing strategies for polymer-based composites for electromagnetic interference (EMI) shielding.

1.1 Scope of the review

Polymer-based EMI shielding materials have been developed using a variety of processing methods, as reported in the literature. Initially, EMI shielding materials are prepared by adding essential filling materials such as conductive, magnetic, and dielectric materials, either alone or in combination, into the polymer matrix. Again, this strategy challenged to achieve the desired EMI shielding performance due to poor dispersion, phase separation within the matrix, and other drawbacks such as high filler content.[26–30] However, the excessive filler content results in the expected shielding but reduces the mechanical properties of the composites.[12] These challenges have resulted in refinement and renaissance of the research approach in polymer nanocomposites toward various structural strategies of nanomaterials and processing strategies of composites. This study also includes glimpses of research exploring biodegradable, longer lasting, and self-healing materials that nurture sustainability in the EMI shielding materials. This review mainly focuses on recent research developments, with a particular emphasis on structural aspects and processing in enhancing the EMI shielding effectiveness of polymer nanocomposites and their underlying mechanisms, as well as some glimpses into the sustainability approaches included in this field. The outcome of this study will help to understand the aspects and material properties such as electrical conductivity (σ), magnetic permeability (μ), dielectric permittivity (ε), and shield thickness (t) that influenced the EMI shielding performance as shown in Fig. 1.

2 The basic theory of EMI shielding mechanism

The EMI shielding effectiveness is the primary metric for determining the performance of an EMI shielding material, which evaluates the EM wave's attenuation by the shield. However, the attenuation of incident EM waves is primarily
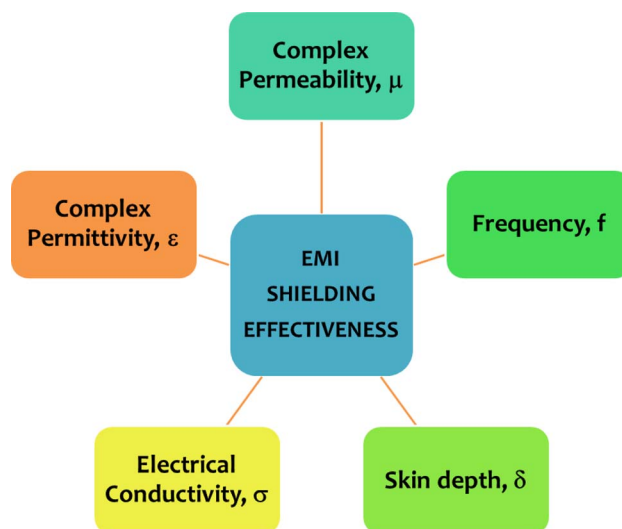

Fig. 1 Factors affecting the EMI shielding characteristics of the polymer composites.

achieved by a combination of reflection, and/or absorption, which exists due to mobile charge carriers and electric and magnetic dipoles within the material.[31] When an EM wave is incident on the surface of the shielding material, an EM wave's energy from the shield will be partly reflected and partly absorbed. The residual energy is neither reflected nor absorbed by the shield but is the energy that emerges from the shield, as shown in Fig. 2.

The attenuation of EM waves occurs mainly by three major mechanisms, namely reflection (R), absorption (A), and multiple internal reflections (MR). A two-port vector network analyzer (VNA) recorded the scattering parameters such as S_{11}, S_{12}, S_{21}, and S_{22} which can be correlated to the reflection, absorption, and transmission coefficients.

$$T = \left|\frac{P_T}{P_I}\right| = \left|\frac{E_T}{E_I}\right|^2 = |S_{12}|^2 = |S_{21}|^2 \quad (1)$$

$$R = \left|\frac{P_R}{P_I}\right| = \left|\frac{E_R}{E_I}\right|^2 = |S_{11}|^2 = |S_{22}|^2 \quad (2)$$

$$A = 1 - R - T \quad (3)$$

where P_T (E_T), P_R (E_R), and P_I (E_I) are the power densities of the transmitted, reflected, and incident EM waves, respectively.

The total EMI shielding effectiveness (SE_T) of a particular material is defined as the efficiency of the barrier material in attenuating EM waves, and it includes losses due to EM waves' reflection and absorption and is expressed in terms of SE_T[31] as follows:

$$SE_T \text{ (dB)} = SE_R + SE_A + SE_M \quad (4)$$

$$SE_T \text{ (dB)} = SE_R + SE_A = 10\log(1/T) = 10\log(1/S_{21}^2) \quad (5)$$

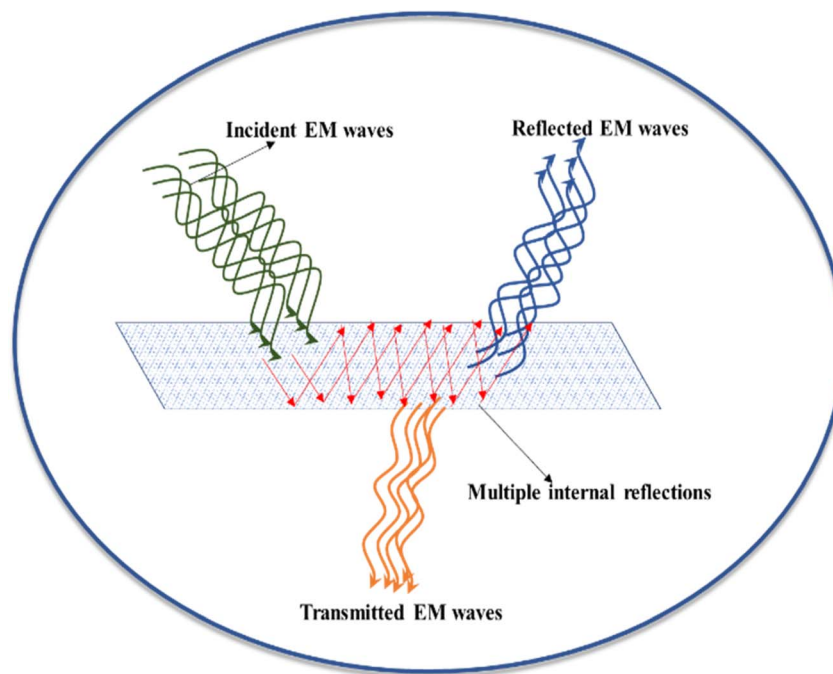$$SE_R = 10\log(1/(1 - R)) = 10\log(1/(1 - S_{11}^2)) \quad (6)$$

Fig. 2 Pictorial depiction of the mechanism of an EMI shielding material.

$$\text{SE}_A = -10 \log(T/(1 - R)) = -10 \log(S_{21}^2/(1 - S_{11}^2)) \qquad (7)$$

where SE_A, SE_M, and SE_R are the shielding effectiveness (SE) due to absorption loss, multiple internal reflection loss and reflection loss. Generally, SE_M was negligible when SE_T was more than 10 dB.[2,3] SE_M can be related to the microwave scattering effect caused by the distribution of conductive and magnetic particles, dielectric polarization, and interfacial polarization, which helps to reduce the intensity of electromagnetic waves entering the material due to the impedance mismatch between air and the material surface.[32]

3 Structure-based strategies of nanomaterials for the fabrication of efficient EMI shielding materials

The electromagnetic theory explains that an impedance match between the shielding material's surface and the incident EM wave results in greater wave penetration. To ensure effective wave interaction, the shield should have adequate electrical conductivity.[4,6,7] Subsequently, a conductive material and/or a hybrid of magnetic–dielectric materials were introduced.[33–38] The dual benefit of the nanofiller produces additional effects such as high multiple-interface polarisation, all of which are useful in increasing shielding effectiveness.[4,7] Previously, several researchers published numerous studies on structure-based strategies for the fabrication of EMI shielding materials, as seen in Table 1. The numerous strategies developed with different structures, such as hybrids (*e.g.*, Fe_3O_4 decorated on graphene nanoparticles or multiwalled nanotubes), core–shell (*e.g.*, $Fe_3O_4@MWNT$), and layered structures, contain various types of nanofillers. A good EMI shielding material should have good complex permeability and permittivity. In the composites, combining these used nanofillers has improved the dielectric loss and the magnetic loss. The increased EMI shielding effectiveness in composites containing structure-

Table 1 EMI shielding values of conductive hybrid structure composites

| Materials	Filler content	Conductivity (S m^{-1})	SE$_T$ (dB)	Frequency (GHz)	Ref.
rGO-CF	0.75 wt%	7.13	37.8	8.2–12.4	39
GNP-MWCNT	10 wt%	9.5	47	20–40	40
CNT/CF	0.35 wt%	0.8×10^{-3}	42	8.2–12.4	41
MNPs@MWCNTs	4 wt%	1070	30–60	0.5–12.0	42
SSF-CNT	3.5 vol%	100	47.5	8.2–12.4	43
Polyamide-6/CNT	0.3 wt%	100	25	8.2–12.4	44
PANI/CNT	25 wt%	1907	27.5–39.2	12.4–18	45
PCL-MWNCT	0.25 vol%	4.8	60–80	0.04–40	46
Copper nanowires-thermally annealed graphene/epoxy	7.2 wt%	120.8	47	8.2–12.4	47
PDMS/0.43 wt% rGO/0.33 wt% AgNW	—	1210	34.1	8.2–12.4	48
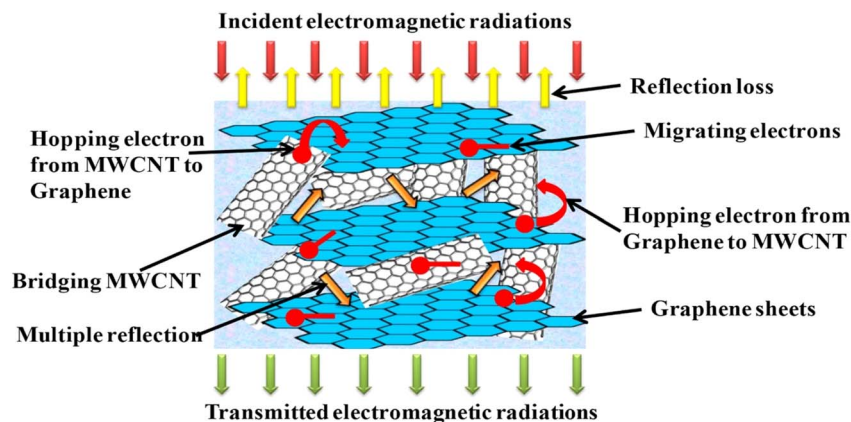
Fig. 3 Schematic representation of the proposed EMI shielding mechanism in PUGCNT nanocomposites. Reprinted with permission. Copyright (2017).[40]

based nanoparticles can be attributed to the combined effects of dielectric losses coupled with the magnetic losses arising due to the presence of structure-based nanoparticles.[49–51] The structure-based strategies can significantly increase the complex permittivity and permeability of polymer composites, thereby increasing the shielding performance of EMI shielding materials.[49–51] Furthermore, the structural refinement of nanofillers includes aspects such as doping/substitution in the entire matrix or one of the fillers, enhancing the current property, or introducing new aspects of additional benefit for the fabrication of an EMI shielding material. Henceforth, this review explains the various types of structure-based composites and their mechanisms adopted to achieve maximum EMI shielding. The main interest in this review paper discusses the role of hybrid nanoparticle combinations, the different layered structure, gradient structures, doped structures, and structures such as foams, aerogels and core–shell structures. The fundamental principles of segregated and template structures are also discussed.

3.1 Hybrid structures

3.1.1 Conductive hybrid structures. The first approach was to create a hierarchical structure containing materials with similar or distinct impedance properties that can attenuate incident EM waves. These structures include combinations of two or more conductive materials in the polymer composite. These hybrid structures were synthesized by physical mixing, synthesis of one filler in the presence of another, or co-synthesis of two or more fillers, which leads to the growth of a decorated structure of one or more fillers on the surface.[39,41] The dual benefit of nanofillers produces additional effects such as high multiple-interface polarisation, all of which are useful in increasing shielding effectiveness. A good EMI shielding material should have good complex permittivity. In the composites, combining these used nanofillers has improved the dielectric loss. The increased EMI shielding in composites containing structure-based nanoparticles can be attributed to the effects of dielectric losses arising due to the presence of

structure-based nanoparticles (Fig. 3). Previously, several researchers published numerous studies on hybrid structures and used them to fabricate EMI shielding materials, as seen in Table 1.

3.1.2 Magnetic and conductive materials' hybrid structures. The second approach is to employ a hybrid structure with a combination of magnetic or dielectric materials and a conductive filler in the polymer composite for the enhancement of EMI shielding efficiency. Subsequently, the addition of conductive materials along with magnetic or dielectric materials generates the dual benefit of nanofillers and produces additional effects such as high multiple-interface polarisation, all of which are useful in increasing shielding effectiveness. In addition, it is well known that two parameters, *i.e.*, magnetic loss and dielectric loss, primarily influence EM wave absorption. In EMI shielding materials, combining a magnetic material with conductive nanofillers has improved the dielectric loss and magnetic loss. In order to create induced magnetic and dielectric losses, a suitable EMI shielding material should have high complex permeability and permittivity. Complex permittivity and permeability are caused by dipole polarization, electronic polarization, natural resonance, magnetic dipoles, magnetic losses, eddy, and hysteresis losses, in which crystal structure, size, and morphology may play a vital role. The increased EMI shielding in composites containing structure-based nanoparticles can be attributed to the combined effects of dielectric losses coupled with the magnetic losses arising from structure-based nanoparticles (Fig. 4).[4,7] Therefore, many researchers have focused specifically on the complex hybrid structure of nanofillers to fabricate an efficient EMI shielding material, which is listed in Table 2.

3.1.3 Magnetic–dielectric–conductive hybrid structures. The third approach is to create a hierarchical structure in the polymer composite containing a combination of magnetic and dielectric materials along with a conductive filler. In these hierarchical structures, decorating magnetic nanoparticles on dielectric materials or *vice versa* facilitated a protective encapsulation of decorated nanoparticles on the surface of other nanoparticles to prevent agglomeration of the nanoparticles.[69]

Previously, researchers reported that magnetic nanoparticles decorated on dielectric nanoparticles have better dielectric properties than dielectric nanoparticles decorated on magnetic nanoparticles because of increased O-vacancy concentration (oxygen vacancy concentration refers to a defect caused by a decrease in oxygen content, leading to an increased number of oxygen vacancies. These vacancies significantly influence the structural, physical, and electrical properties of the material in dielectric nanoparticles of larger grains and O-vacancy-induced enhancement in interfacial polarisation between the dielectric nanoparticles and magnetic nanoparticles, respectively.[70–73]

Recent studies have investigated the use of dielectric materials, including SnO_2, TiO_2, ZrO_2, ZnO, Al_2O_3, carbon materials, and polymers, as a dielectric source to impart dielectric losses and their use alone or in combination with magnetic and conductive materials.[74] For example, Biswas et al. synthesized graphene oxide sheets decorated with $BaTiO_3$ and Fe_3O_4 nanoparticles. These nanoparticles are combined with modified MWNT and embedded in the polycarbonate (PC)/polyvinylidene fluoride (PVDF) matrix. The nanocomposite reported SE_T values of 32.5–35 dB over the frequency range of 12–18 GHz. It can be observed that the composites demonstrated an increase in SE_T

values due to the synergistic effect of hybrid lossy materials and selective localization of graphene oxide (GO) in PC and MWNT in PVDF, which retains the electrical conductivity of composites.[74] The authors also fabricated composites through multilayer assembly, having outer layers with a modified $BaTiO_3$/Fe_3O_4 co-doped GO/modified MWCNT/PC/PVDF composite and inner layers with MWCNT/PVDF modified in the composite.[74] The authors also reported that the SE_T values of composites fabricated through multilayer assembly further increased to 46 dB over the frequency range of 12–18 GHz.

Jin et al. synthesized a hybrid structure made of graphene nanoplates along with Fe_3O_4 decorated on $BaTiO_3$ (GFBT) in a two step hydrothermal process. The $BaTiO_3$ particles of 20 nm are primarily coated on the Fe_3O_4 nanospheres forming the hybrid structure of Fe_3O_4 and $BaTiO_3$. The hybrid structure containing $BaTiO_3$/Fe_3O_4 nanoparticles of about 200 nm diameter anchored on the surface of graphene was used along with MWNT in methyl vinyl silicone rubber. The composite containing 16 wt% filler loading with a ratio of 1 : 5 of MWNT : GFBT exhibited SE_T values of 26.7 dB in the frequency range of 1–20 GHz for a sample thickness of 2.6 mm.[75] Sambyal et al. reported an encapsulated polypyrrole composite with the
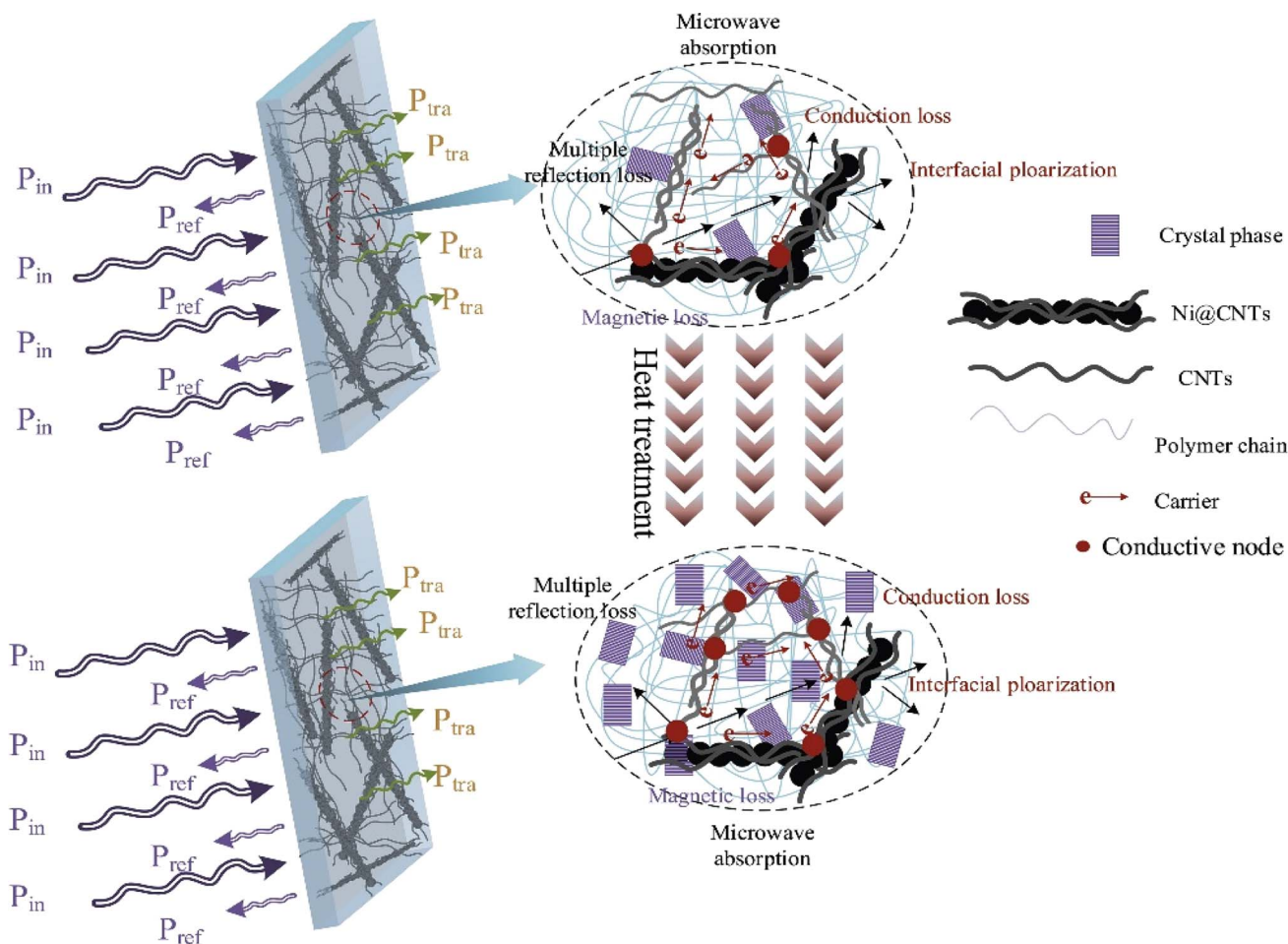

Fig. 4 A schematic illustration of the distribution of the conductive filler in PVDF/CNTs/Ni@CNTs flexible composite films before and after heat treatment. Reprinted with permission. Copyright (2019).[52]

Table 2 EMI shielding values of conductive and magnetic hybrid structure composites

Materials	Synthesis method	Conductivity (S cm^{-1})	Thickness (mm)	Polymer matrix	SE$_T$ (dB)	Frequency (GHz)	Ref.
PANI/15 wt% BaFe$_{12}$O$_{19}$ (BF)	Co-precipitation	0.34	2	PANI	19.7	2–18	53
PANI/28 wt% Mn$_{0.5}$Zn$_{0.5}$Fe$_2$O$_4$			2	PANI	6–20	0.03–1	54
3% Graphene decorated with nickel NPs	Co-precipitation	3.10×10^{-4}	1	Polybenzoxazine	>20	8.2–12.4	55
10 wt% CNT/12 wt% Ni@CNT	Magnetic field-supported solvothermal process	2.57	0.5	PVDF	51.4	12.4–18	52
rGO-FeCo-diamine monomer 4,4′-diamino diphenyl methane, MWCNT	In situ reduction using a solvothermal process	1×10^{-3}		PVDF	41	12.4–18	56
10 wt% Fe$_3$C-carbon	Carbonization of melamine and iron salt			PVDF	35	14–18	57
90 : 10 ratio of Fe$_3$O$_4$ and carbon black (CB)		10		Natural rubber	14.7–23.1	1–12	58
0.25 vol% Fe$_3$O$_4$-MWCNT			5	Polycarbonate (PC)/PVDF	38	18	59
0.25 vol% Fe$_3$O$_4$-MWCNT			5	PC/PVDF	30–36	8–18	60
0.15 vol% NiFe$_2$O$_4$-MWCNT			5	PC/PVDF	19.7	2–18	60
0.28 vol% CoFe$_2$O$_4$-MWCNT			5	PC/PVDF	6–20	0.03–1	60
Modified Gr nanoplatelets and MWCNT-Fe$_3$O$_4$				Polyurethane	27.5	8–12.4	61
Fe$_3$O$_4$-CNT		9×10^{-3}	1.1	PVDF	32.7	18–26	62
Fe$_3$O$_4$-GNP		2×10^{-2}	1.1	PVDF	35.6	18–26	62
rGO@Fe$_3$O$_4$-MWCNT		1.8×10^{-3}	5	PC/polystyrene	>30	8–18	63
0.5 wt% rGO deposited with carbon fiber-Fe$_3$O$_4$-9 wt% modified rGO		11.04	7	Epoxy matrix	>30	8.2–26.5	64
rGO-Fe$_3$O$_4$		7×10^{-4}		PC matrix	28	8–18	65
rGO-Fe$_3$O$_4$		4×10^{-4}		PC matrix	33	8–18	65
4 wt% CNT-5 wt% rGO-Fe$_3$O$_4$				PC matrix	43.5	8–12.4	66
45 wt% NiFe$_2$O$_4$-5 wt% rGO		2.16×10^{-12}	2	Propylene	28.5	5.8–8.2	67
NiCoFe$_2$O$_4$ (NCF)-CB		1.513×10^{-4}	1.5	Polyvinyl alcohol (PVA)	27	8–18	68

combination of rGO, Fe$_3$O$_4$ and barium strontium titanate (BST) nanoparticles. The BST/rGO/Fe$_3$O$_4$ (BRF) hybrid was synthesized by co-precipitation. In this process, the precursors

rGO and BST nanoparticles were added to the precursor solution of Fe$_3$O$_4$, thus forming the hybrid structure of nanoparticles. The hybrid composite showed an EMI SE of around 48 dB for a thickness of 2.5 mm in the X-band frequency range (Fig. 5).[76]
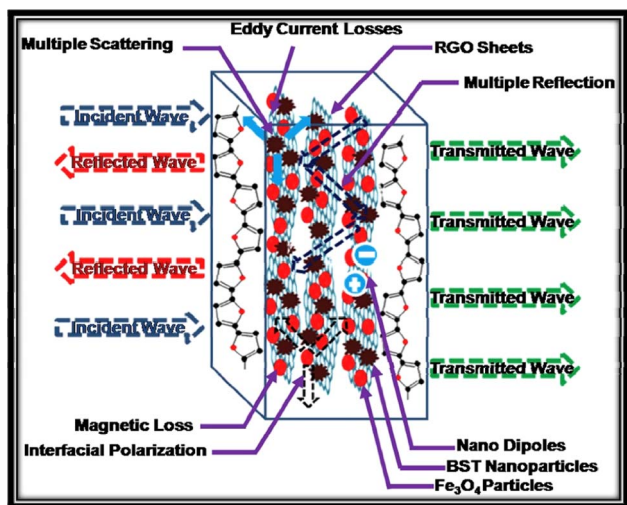
3.2 Layered structures

The layered structures provide ultralight, low density, flexible, scalable, and highly conductive micrometer-thick EMI shields that can be made using standard polymer processing methods for flexible, wearable, and smart electronics. The production of multifunctional EMI shields is the major challenge to be addressed. The industries require EMI shields that not only limit the detrimental impacts of EM waves but also have exceptional mechanical and thermal properties.[77,78] The second major challenge is the necessity to manufacture EMI shields that absorb a large amount of the incoming EM waves. Furthermore, several research studies have only focused on the development of highly conductive EMI shields that rely heavily on EM wave reflections. However, this strategy is undesirable for military and medical applications that demand a high level of EM wave absorption with minimum reflections. Indeed, EM waves reflected from a conductive EMI shield can serve as

Fig. 5 Schematic representation of a possible mechanism of EMI shielding in the PBRF composite. Reprinted with permission. Copyright (2018).[76]

Table 3   The layered structure composites and their EMI shielding effectiveness values

Materials	Thickness (mm)	Conductivity (S m^{-1})	SE$_T$ (dB)	Frequency (GHz)	Ref.
PP-MWCNT/PP-MA/10 wt% PVA-2 wt% MWCNT	1	0.03	36.7	1–2	80
PP-MWCNT/PP-MA/10 wt% PVA-2 wt% Gr sheets	1	21	24.5	1–2	80
Cellulose/PET oxide-CNT	0.15	20	35	8–12	81
PPEK/MWNT	11	39	61.5	8–12	82
MWNT/PMMA	0.3	1.5	40	8.2–12.4	83
SWNT/cellulose	0.03	—	40	12–18	84
PVDF/GNP-Ni-CNT	0.6	0.15	46.4	12.4–18	85
T-ZnO/Ag/WPU	0.25	63 500	87	8.2–12.4	86
GO/PHDDT	0.02–4	—	37.92	8–12	87
CNT/BN/rubber	1.4	98	31.38	8–12	88
PVDF-MWCNT-Mn-Fe$_3$O$_4$/Ni-C-PVDF	0.6	—	58	12–18	89
PC/PVDF with MWCNT-Fe$_3$O$_4$	0.9	1.1×10^{-4}	64	12–18	90
PVDF/CoNi/MWNT	0.95	1	41	20–40	91
Ni@nylon mesh/PP	2.5	2.26	50.6	8–12	92
PC/ethyl methyl acrylate/MWCNT/GNP	—	1.91×10^{-1}	34	8.2–12.4	37
PANICNPS	10	7.6×10^{-1}	10–20	8	93
Fe$_3$O$_4$@rGO/T-ZnO/Ag/WPU	0.5	22 700	87.2	8–12.4	94
FeCo@rGO/Ag/WPU	0.3	1428.57	50.5	2–18	95
FeCo@rGO/Ag/NWF/WPU	0.1	60 000	77.1	2–18	96
Silicon rubber/Ag@HGMs/Fe$_3$O$_4$@CNT	2	279.3	59.39	8–12.4	97
FeCo@rGO/EbAg/WPU	—	—	84.8	8–12.4	98

a secondary source of EMI, affecting the operation of neighbouring electronics.

The manufacturing of multilayer EMI shields has recently been suggested as a potential strategy to decrease reflection and increase EM wave absorption. A multilayer structure comprising suitable nanomaterials and polymers was used to create multifunctional EMI shields with excellent EMI shielding properties. Furthermore, it has been demonstrated in several investigations that a layered structure of conductive and magnetic materials may significantly improve the absorption component of the shielding and, to a large degree, the overall EMI shielding effectiveness (EMI SE) of developed structures. This study concisely described the main ideas of EMI shielding, as well as the underlying shielding mechanisms of multilayer shields, and then provided a complete evaluation of fascinating multilayer shield research.

The current state-of-the-art is to prepare a multilayer structure EMI shielding material with softness, durability, rapid thermal dissipation, and desirable resilience and endows the composites with excellent shielding effectiveness.[79] Layered structures, such as sandwich structures, have been proven to be an effective strategy for attenuating EM waves. Furthermore, the layer-by-layer (LbL) assembly is a reliable process for making thin-film materials, which is used to build the layered structure composites required for EMI shielding applications. Therefore, this process was utilized to manufacture multilayer structured coatings for high-efficiency EMI shielding.[79] The multilayer structure, comprising various conductive materials with different impedances or conductive and/or magnetic materials, creates unique interfaces among the materials that generate multiple internal reflections for EM waves, thereby boosting EMI shielding performance.

In addition, a few efforts have been made to produce highly efficient multilayer composites for EMI shielding applications. These studies reported that multiple internal reflections, along with prevailing shielding mechanisms, impedance mismatch, and dielectric losses contribute to the improvement of the shielding effectiveness. The preparation methods for producing thin-film composites in the form of multilayer stacks have been
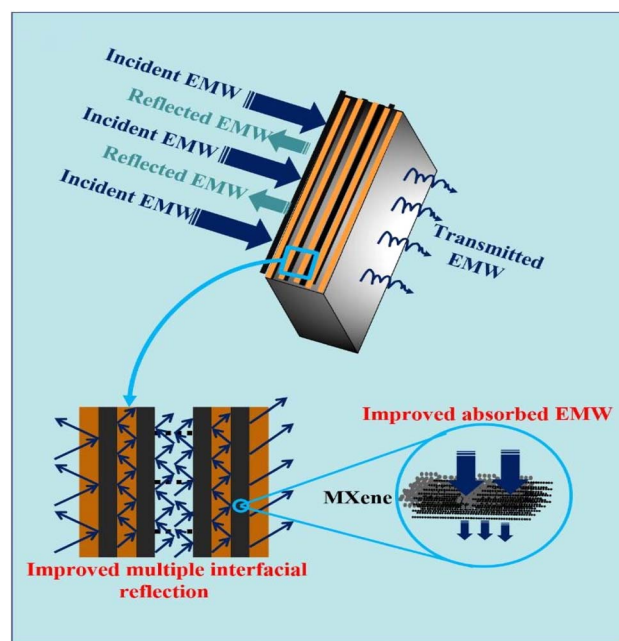

Fig. 6   Schematic of electromagnetic microwave dissipation in the PVA/MXene multilayered films. Reprinted with permission. Copyright (2020).[78]
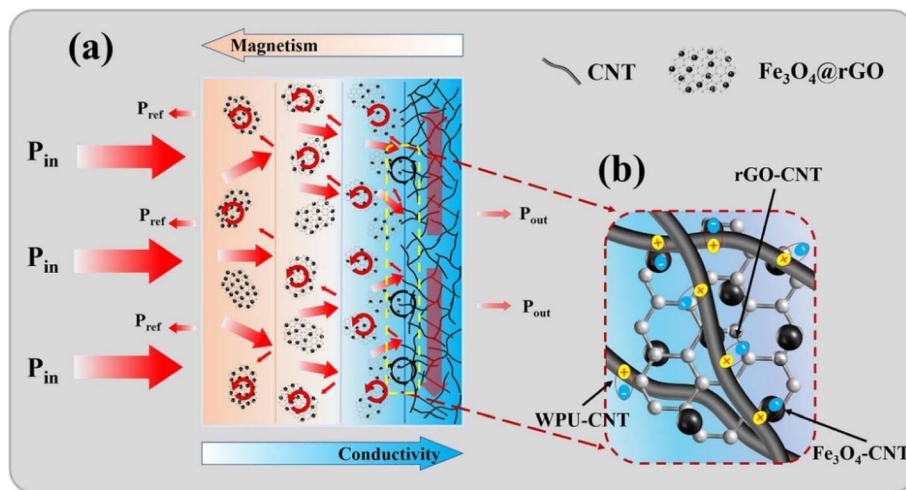
Fig. 7 (a) EMI shielding mechanism of the $Fe_3O_4@rGO/MWCNT/WPU$ composite. (b) Polarization relaxation loss mechanism of the interface between $Fe_3O_4@rGO/WPU$ and MWCNT/WPU. Reprinted with permission. Copyright (2020).[99]

developed, and considerable work has already been published and is listed in Table 3. Layered structure composites are categorized based on a physical assembly of layers, self-assembled layered or *in situ* layered structures with different combinations of fillers and different matrices (Fig. 6).

3.3 Gradient/graded structures

EMI shielding materials that are lightweight, flexible, and readily functionalized offer greater application possibilities in a wide range of applications such as portable electronics and wearable materials. To achieve this, gradient layered structures have been created by layering polymer nanocomposites and increasing or decreasing the concentration of fillers layer by layer from the EM wave incident layer.[6] This gradient structure strategy can facilitate the creation of an extremely efficient EMI shielding material with low reflection. However, this gradient structure is mostly constrained by the manufacture of films and solid composites; few studies have been undertaken on creating gradient structures for composites using simple protocols (Fig. 7).

Xu *et al.* have prepared flexible waterborne polyurethane (WPU) composite films by developing gradient structures as the density difference among $rGO@Fe_3O_4$ and T-ZnO/Ag nanoparticles.[94] These gradient structures demonstrated significant EMI shielding performance of 87 dB with as low as 39% reflection power. The reflection power value of the $Fe_3O_4@rGO/MWCNT/WPU$ composites may be reduced to 27%.[94] This

suggested that the gradient structure containing both electric and magnetic materials reduced their reflection power in the gradient structure by regulating rGO content. H. J. Im *et al.* designed a multilayer graded structure by incorporating fillers of GNP and Ni in the polymethyl methacrylate (PMMA) matrix. Firstly, the Ni was reduced onto GNP and then incorporated into PMMA.[100] The gradient structure consisted of 0.83 mm thick three layers, where the top layer containing the concentration of GNP/Ni filler loading increased by 20 wt%. The intermediate layer contains 30 wt% filler loading, and the bottom layer contains 40 wt% filler loading. The gradient structure exhibited an EMI SE value of 61 dB over the X-band frequency range of 8–12.4 GHz. The gradient structure has demonstrated 3 orders higher thickness than a monolayer of 2.5 mm thickness containing 30 wt% GNP/Ni filler loading. The authors attributed the abrupt increase in filler loading by 10 wt% to have helped to develop a conductive network structure between layers in the direction of propagation of EM waves. It can create multiple additional internal reflections between the stacked layers. It can also be observed that the top layer containing lower filler loading supports better impedance matching and reduces surface reflections. It can enhance the absorption of EMI waves in the gradient structure.[100] A. Sheng *et al.* designed a conductive gradient structure for reducing reflections in the hybrid system.[99] The gradient structure was constructed by three layers of $Fe_3O_4@rGO$. The rGo filler loading was increased from the top layer to the bottom layer in the gradient structure and the

Table 4 Gradient structure composites and their EMI shielding effectiveness

Materials	Thickness (mm)	Conductivity (S m^{-1})	SE$_T$ (dB)	Frequency (GHz)	Ref.
GNP/Ni/PMMA	2.5	—	61	8–12	100
WPU/Fe$_3$O$_4$@rGO/MWCNT	0.8	3.75	35.9	8–12	99
3 Layers of SWCNT/vinylidene fluoride	1.12	—	−6	35	101
Ti$_3$SiC$_2$-γ-Al$_2$O$_3$/SiC	46	1000	50	8.2–12.4	102
CNT/SiO$_2$	5	—	−30	8–12	103
Fe/Al-Fe/Fe	1	0.16	70–80	0.03–1.5	104

final layer containing MWNT in the WPU matrix. The gradient structure exhibited an EMI SE value of 35.9 dB for the composite containing the 11.2 wt% Fe_3O_4@rGO-30 wt% MWNT-WPU composite within the X-band frequency range of 8–12.4 GHz.[99] The composites containing gradient structures have enhanced the EMI SE value and are listed in Table 4.

3.4 Doped structures

The doping of EMI shielding materials and their enhancement strategies can be divided into three categories: (i) doping excellent conductive nanofillers, (ii) increasing the loading content of nanofillers and (iii) approaching the homodispersity of nanofillers in the polymer matrix. Despite substantial research on the fabrication of EMI shielding materials, the true potential of doped structures for this use has yet to be investigated. The doping of nanofillers such as graphene helps to retain the sp^2 electronic structure by increasing the electrical

conductivity of doped structures.[105] Currently, n-type doping of carbon-based nanofillers such as graphene with heteroatoms such as nitrogen was proposed as a viable method for recovering graphene's electronic properties. Furthermore, sulfur is a comparatively recent n-type dopant, and its ability for applications apart from electrochemistry has yet to be thoroughly investigated. Zhou *et al.* and Denis *et al.* found that S-doped graphene produces a thiophene-like structure that has a favorable effect on graphene's magnetic and electronic properties.[106–108] This review reported that doped nanofillers in a laminated structure exhibit considerably larger EMI shielding effectiveness than the undoped laminate at minimal thicknesses. This observation is attributed to the n-doping effect of nanofillers, which improves the electrical conductivity of doped structures (Fig. 8). The composites containing doped nanostructures have enhanced the EMI SE value and are listed in Table 5.
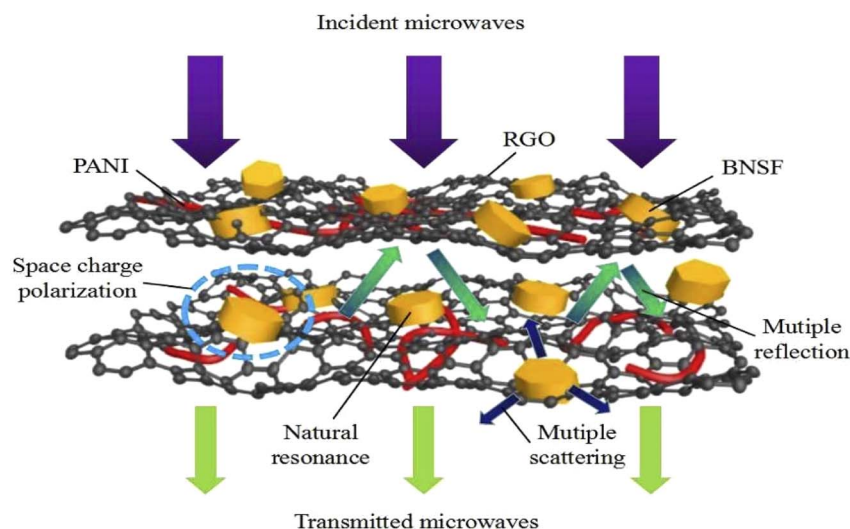
Fig. 8 Schematic representation of the microwave attenuation mechanism in RGO/PANI/BNSF nanocomposites. Reprinted with permission. Copyright (2019).[109]

Table 5 Doped structure composites and their EMI shielding effectiveness

Materials	Thickness (mm)	Conductivity (S m^{-1})	SE$_T$ (dB)	Frequency (GHz)	Ref.
$Ti_3C_2T_x$/c-PANI	0.04	2440	36	8–12	110
RGO/PANI/BNSF	2.90	—	50.5	2–18	111
p-TSA/PANI/GNPs	1.5	57.5	14.5	8–12.4	112
PANI/CSA-coated CNF	0.088	38.5	30	0–15	113
MWCNTs/sub-SF/PANI	5	—	36	8–18	114
PC/sub-G/MWCNT	5	6.1×10^{-2}	33	8–18	65
N_2-doped graphene nanosheet – epoxy	2.4	—	40	8–12.4	115
Fe_3O_4/CCTO/P-gC$_3$N	1	—	30	8–12.4	116
PANI/Ni-Cd-ferrite	2.3	4470	42.7	8–12.4	117
Silicone rubber/POE/IL-MWCNT	1.2	0.14	25	8–12.4	118
TPU/sub-G	1	10	25	8–12.4	119
SBR/IL-MWCNT	5	10	35	2–18	120
PS/IL-MWCNT	1	0.01	7	8–12.4	121
Pyrrole/Nd-Co	2	—	15	8–12.4	122

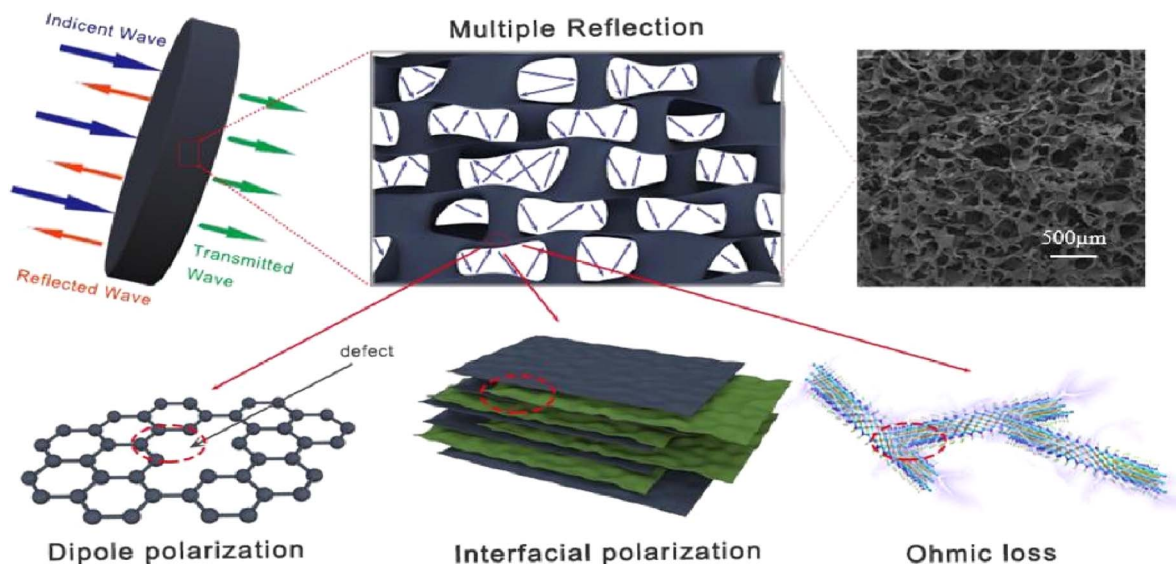**Fig. 9** Possible electromagnetic shielding mechanism of the $Ti_3C_2T_x$/RGO/ANFs hybrid aerogel. Reprinted with permission. Copyright (2022).[128]

3.5 Aerogel composites

Aerogels have emerged as one of the most interesting materials of the late 20th century. The innovative processing technique yields aerogels with remarkably high porosity, large specific surface area, low density, high dielectric strength, and low thermal conductivity, making it possible to utilize these materials in various applications such as aerospace, biomedical devices, energy storage, EMI shielding materials, sensors, and coatings.[123] Since Kistler invented the aerogel with silica, aerogels have been created from a wide range of materials, that includes metal oxides, biopolymers, resins, *etc.*[124] Furthermore,

a range of nanomaterials can be added into the aerogel matrix to construct composites with aerogels. Moreover, an aerogel network has pore diameters in the order of nanometers. The further addition of nanomaterials into an aerogel produced a composite with superior functional properties including increased specific surface area, improved mechanical strength, and better thermal and electrical conductivity.[125]

Since this first use of carbon nanomaterials in the production of an aerogel structure, the utilization of a variety of nanomaterials for the development of high-performance aerogel structures has grown exponentially. For example, carbon

Table 6 Aerogel composites and their EMI shielding effectiveness

| Materials	Type	Method	Conductivity (S m^{-1})	SE$_T$ (dB)	Frequency (GHz)	Ref.
PDMS/0.21 wt% rGO/0.07 wt% SWCNT	Aerogel foams	Freeze drying method	120	31	8.2–12.4	130
0.51 wt% CNT/cellulose	Template	Ice-template freeze drying method	38.9	51	8.2–12.4	131
0.74 vol% $Ti_3C_2T_x$/graphene/epoxy	Nanocomposite	Hydrothermal assembly and freeze-drying	695.9	50	8.2–12.4	132
1.95 wt% PDMS/reduced graphene	Flexible foams	Freeze drying	65.6	43.6	8.2–12.4	133
Polyurethane (WPU)/silver nanowire (Ag-NW)	Flexible nanocomposites	Freeze drying	587	64	8.2–12.4	134
0.8% Graphene/epoxy	Nanocomposite	Freeze drying and thermal annealing	980	32	8.2–12.4	135
0.2 wt% TAGAs/epoxy	Nanocomposite	Freeze drying and thermal annealing	96	25	8.2–12.4	135
6.1 wt% MXene ($Ti_3C_2T_x$)/sodium alginate (SA)	Aerogel	Freeze drying	2211	48.2	8.2–12.4	136
Nacre-mimetic graphene (aerogel)/PDMS	Aerogel	Bidirectional freezing and freeze drying	0.5	65	8–12	137
1.64 wt% $Ti_3C_2T_x$ MXene/epoxy	Foam	Sol–gel followed by freeze drying	184	46	8–12.4	138
0.33 wt% Graphene/phenolic resin/epoxy resin	Aerogels	Hydrothermal	73	35	8–12.4	139
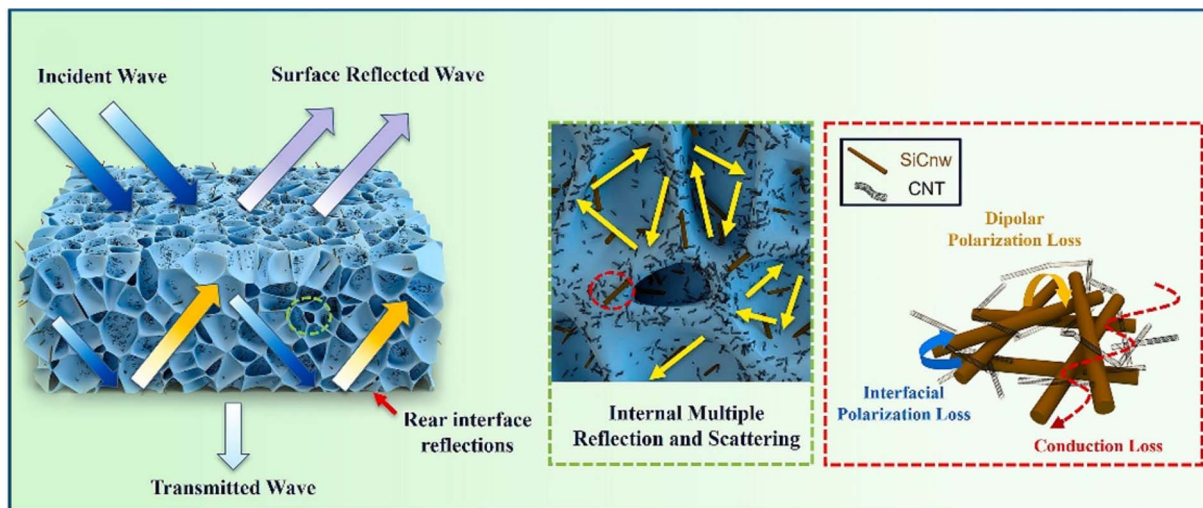
Fig. 10 Schematic illustration of EM wave dissipation in the PVDF/CNT/SiCnw composite foams. Reprinted with permission. Copyright (2023).[140]

nanomaterials such as carbon nanotubes, graphene, and carbon nanofibers have been incorporated into aerogels to improve the electrical conductivity and performance for applications such as supercapacitors, sensors, and batteries[126,127] (Fig. 9).

In other earlier works, the lightweight 3D structure design is a primary prerequisite in EMI shielding applications. The actual EMI SE for lightweight porous materials was determined in terms of specific shielding effectiveness (SSE) and absolute shielding effectiveness (ASE), which define the accurate shielding performance of the material by considering three factors: EMI SE, density (ρ), and thickness (t), which are calculated as follows,

$$SSE = SE_T/\rho \; dB \; cm^3 \; g^{-1}$$

$$ASE = SSE/t = SE_T/\rho t \; dB \; cm^2 \; g^{-1}$$

The pores developed in the lightweight 3D structure decrease the density of the material and are also supposed to increase multiple internal reflections of EM waves, increasing EMI SE values. Porosity has been integrated into the material to reduce the density of the EMI shielding materials to get the best of both SE and lightweight, and the impact of porosity on the properties and structure of porous materials has been adequately studied. Hu *et al.* investigated multifunctional aerogel films made with Kevlar fiber, carbon nanotubes (CNT) as reinforcing fillers, and

Table 7 Foam composites and their EMI shielding effectiveness

Materials	Thickness (mm)	Conductivity (S m^{-1})	SE$_T$ (dB)	Frequency (GHz)	Ref.
TG-CN/PMMA	2	1	34	8.2–12.4	144
RG-CN/PMMA	2	0.1	19.5	8.2–12.4	144
GN-CN/PMMA	2	0.8	26	8.2–12.4	144
PVDF/Ni-chains	2	0.01	26.8	8.2–12.4	145
Silicone rubber/MWCNTs/Fe$_3$O$_4$	2	14.6	27.5	8.2–12.4	146
GO/NF/epoxy	0.5	150	65	1–3	147
fMWCNTs/CTBN/epoxy	2	0.43	22.90	12–18	148
PMMA/GNPs-MWCNTs	2	0.1	36	8–12	149
CNTs/PMMA laminated	2	—	36	8–12.4	150
GNPs/PMMA	2			8–12.4	151
EP/ZrP-MWCNT	2.2–2.5	3.02×10^{-4}	20.5	12–18	152
PMMA/Fe$_3$O$_4$@MWCNTs	2.5	2×10^{-4}	16	8.2–12.4	153
PMMA/MWCNT	3	—	—	8.2–12.4 GHz	154
Microcellular epoxy/MWCNT	2.8	1×10^{-7}	9	12–18 GHz	155
PC/GNP	5	1×10^{-7}	39	8–12 GHz	156
PVDF/MWCNT	1.7	0.44	34.1	18–26.5 GHz	157
PVDF/10 wt% GNP	3	0.52	37.4	26.5–40 GHz	158
Silicone/30 wt% o-MWCNTs	6.4	—	73	12.4–18 GHz	159
PU/31.3 wt% rGO	2.5	—	−50.8	2–18 GHz	160
Epoxy/0.94 vol% AgPs/0.44 vol% rGF	3	45.3	58	8.2–12.4 GHz	161
PDMS/2.7 wt% GF/2.0 wt% CNTS	2 ± 0.05	31.5	833	8.2–12.4 GHz	162

hydrophobic fluorocarbon resin as a polymer matrix. The final material comprises self-cleaning properties due to the hydrophobic surface nature of the film, having good electrical conductivity leading to joule heating properties and good EMI shielding properties of 54.4 dB at a thickness of 546 μm in the X-band region (8–12 GHz)[129] (Table 6).

3.6 Foams

Polymer foams have attracted great attention in designing EMI shielding materials due to their advantage of being lightweight, while the unique porous structure can effectively absorb EM waves by extending the travel path.[25] Foam composites demonstrated absorption-dominated shielding phenomena, which meets the present standards of EMI shielding applications. Furthermore, conductive polymer foams, carbon foams, inorganic metal foams and MXene foams are gaining popularity for use in EMI shielding applications. The primary goal of this review is to study the current state of research in the design of polymer composite foams as EMI shielding materials (Fig. 10).

Zhang *et al.* used subcritical CO_2 ($scCO_2$) as a physical foaming agent to fabricate a graphene-reinforced PMMA composite. The established multi-interface microporous structures have the potential to improve shielding effectiveness by allowing for multiple internal reflections and resolving the composites' pervasive brittleness.[141] Furthermore, Zhang *et al.* fabricated three-dimensional (3D) compressible foam with conductive MXene sheets. The prepared conductive network was covered with a thin layer of elastic polydimethylsiloxane (PDMS) to increase mechanical robustness.[136] After 500 compression–release cycles, the PDMS-coated foam achieved a superior EMI SE value of 48.2 dB, demonstrating its remarkable ability for compressible and robust EMI shielding gaskets. Gupta *et al.* formulated a 2,20-azobisobutyronitrile (AIBN), a chemical blowing agent used to prepare the CNT-PS foam composite. When heated, AIBN decomposed and released

nitrogen gas inside the composite structure, providing adequate EMI shielding efficiency.[142] Shen *et al.* used a modified water vapour-induced phase separation method to create porous PVDF/MWNT/graphene composites.[143] Furthermore, syntactic foam is a foam composite of hollow fragments distributed in a matrix. Two techniques have been used, including the use of conductive hollow particles as fillers for syntactic foams and the addition of excess conductive filler to syntactic foams. Furthermore, the template process has been illuminated to manufacture foam-based shielding materials due to its ease of operation, controllable structure, and diverse alteration. The polymeric composition can be coated on the pre-constructed conductive foam in reverse on the composite foam for EMI shielding. Foam-based structures were boosting multiple reflections and so on. Similarly, processing aspects like modifications in blending techniques, layered assembling, and even irradiation process boost EMI shielding through uniform dispersions, sequential attenuation, *etc.* Herein, we attempt to bring in a consolidated review of recent research with insights on the structural and processing-based approaches and their combinations and their underlying mechanism that has boosted the EMI shielding performance. Several researchers prepared various foams and determined their EMI shielding effectiveness which are listed in Table 7.

3.7 Core–shell structures

Core–shell nanoparticles are a special class of nanostructured materials that have attracted a great deal of interest in the last two decades due to their unique characteristics and wide range of applications. A variety of "core–shell" nanostructures with tailorable characteristics may be generated by properly regulating the "core" and "shell", which can be utilised to build materials for EMI shielding. The primary goal of this study is to emphasise the fundamental notion of EMI shielding materials that have been discussed in the literature for various systems, as
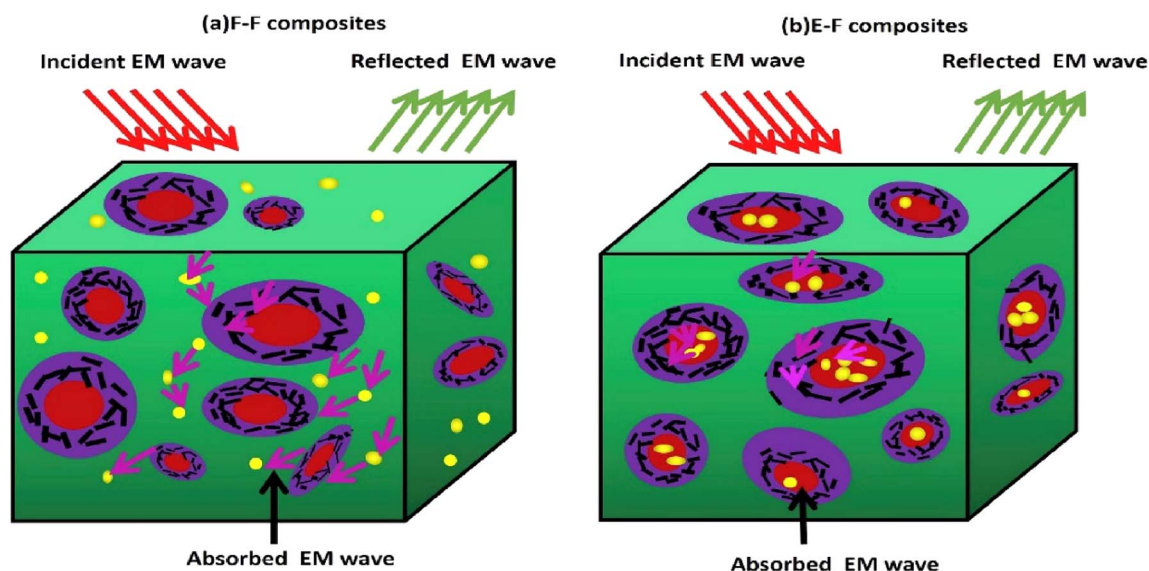

Fig. 11 Cartoon illustrating the EMI shielding mechanism for the composites (a) F–F composites [PVDF–Fe_3O_4], (b) E–F composites [HDPE–Fe_3O_4]. Reprinted with permission. Copyright (2018).[165]
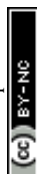
Table 8 Polymer composites containing core and shell particles and their EMI shielding effectiveness

Materials	Thickness (mm)	Conductivity (S m^{-1})	EMI SE (dB)	Frequency (GHz)	Ref.
PVDF/FeCoSiO$_2$@MWNT (10 wt%)	3	—	35	2–18	164
Fe$_3$O$_4$@C@PANI (Fe$_3$O$_4$@C : PANI:1 : 9)	1	4.06×10^{-1}	65	2–8	166
FeCo@SiO$_2$@PPy	2.1	—	65.17	2–18	167
PVDF/F$_3$O$_4$ (3 wt%)@SiO$_2$@MWCNTs (10 wt%)	0.6	2×10^{-3}	40	12–18	168
fMWCNT-Fe$_3$O$_4$@Ag/epoxy (MWCNT : Fe$_3$O$_4$:9 : 1)	2	28	35	8.2–12.4	169
F$_3$O$_4$ (20 wt%)@SiO$_2$@PPy	0.27	71	32	8–12.4	170
PVDF/PS/HDPE/MWCNTs (70/20/10/1 vol%)	2.5	1.2	25	8–12.4	165
Ni@SnO$_2$@PPy	3.5	14.28	30.1	2–18	171
Co@C-PVDF	—	—	25.49	8–12.4	172

well as various synthetic and manufacturing methodologies for creating acceptable EM attenuation.

In this approach, the prepared core@shell may be made up of two distinct types of substance, inorganic@organic and *vice versa*, or the same type of substance with different structures, such as inorganic@inorganic or organic@organic. The construction materials or the core or shell thickness ratio can modify the properties of these materials. The main drawback in the preparation of core@shell particles is a complex and time-consuming strategy.

Previously, a few researchers claimed that reinforcing core@shell particles in the polymer matrix can improve the polymer's complex permittivity and permeability. It can also help with impedance matching, which occurs as a result of several relaxation mechanisms in the polymer. In the core and shell nanoparticles with a specific thickness of shells, an unexpected dielectric behavior that strengthened EMI shielding effectiveness was demonstrated. On the other hand, Liu *et al.* presented the well-defined shells, unique morphological characteristics, desirable magnetization, large surface area, and large porosity of the yolk-double-shelled Fe$_3$O$_4$@SnO$_2$ particles which significantly enhanced the EMI SE characteristics of the composite.[163] The significant increase in the absorption of the EM wave of the composite containing Fe$_3$O$_4$@SnO$_2$ can be attributed to the individual shells in the yolk–shell structure, which provided the synergistic effect between the core containing magnetic Fe$_3$O$_4$ and the dielectric shell containing SnO$_2$ nanoparticles. Zhang *et al.* chose polyaniline (PANI) and bagasse fiber (BF) to develop a heterostructure by insulating PANI over the fiber surface to form a conductive lightweight material. The properties depend on the total coverage of PANI on the fiber surface as the higher the PANI content the greater the electrical conductivity. The material showed good complex permittivity because PANI improves dipolar polarization and conductivity.[81]

The exceptional EMI shielding properties of these nanoparticles were attributed to the complementary activity of the dielectric loss and the magnetic loss generated in the composite due to core–shell structure nanoparticles. Owing to the presence of the conductive shells or core, the eddy current effect was effectively minimized, and anisotropy energy was increased in the core–shell structured nanoparticles.[164] Owing to the presence of the magnetic core or shell, magnetic losses such as natural ferromagnetic resonance loss, domain wall resonance loss, and hysteresis loss are produced, which usually play an important role in the enhancement of EMI shielding effectiveness (Fig. 11).

In general, composites containing core@shell nanoparticles are receiving great attention due to their potential advantages such as core-corrosion safety, interfacial polarization, complementary behavior, and confinement effect. Furthermore, a wide range of composites containing core@shell nanoparticles with reasonable attenuation of EM waves have been investigated and data are listed in Table 8.

3.8 Segregated structures

The conductive polymer composites were incorporated with large loadings of conductive fillers into the polymer matrix to form a percolated network structure which increases the electrical conductivity of the polymer composite. This conventional approach in the fabrication of polymer composites improves their density but is not a cost-effective or industrially viable method. Owing to such issues, the segregated structure facilitates the formation of a percolated network with low filler loadings in the fabrication of polymer composites among all
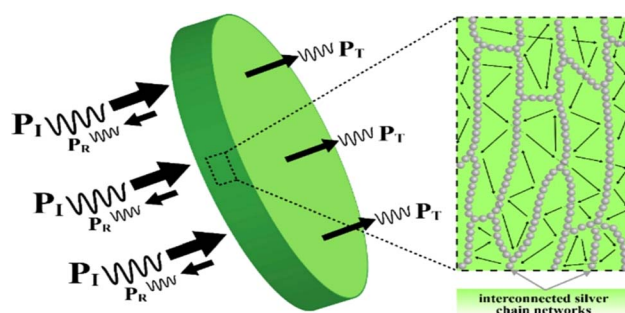

Fig. 12 Schematic EMI shielding mechanism for the PLA/Ag composites with novel segregated electrically conductive Ag networks. Reprinted with permission. Copyright (2018).[173]

Table 9 Segregated structure composites and their EMI shielding effectiveness

Materials	Filler content	Thickness (mm)	Conductivity (S m^{-1})	SE$_T$ (dB)	Frequency (GHz)	Ref.
PP/CNT/CB foam	5 wt%	0.26	6.67×10^{-1}	72.23	8.2–12.4	176
PS/MWNT	7 wt%	1.8	11	26.3	8.2–12.4	177
PDMS/MWNT/SGM	SGM-30 vol%; MWNT-3 vol%	2.7	50	55	8.2–12.4	178
PDMS/MWNT/HGM	HGM-40 vol%; MWNT-3 vol%	2.7	47.5	53	8.2–12.4	178
PMMA/rGO	2.6 vol%	2.9	91.2	63.2	8.2–12.4	179
PMMA/rGO/magnetite	rGO-1.1 vol% Magnetite-0.5 vol%	2.9	—	29	8.2–12.4	179
NR/Fe$_3$O$_4$@rGO	78% Fe$_3$O$_4$ 10 phr rGO	1.8	6.1	42.4	8.2–12.4	180
NR/rGO	10 phr rGO	1.8	8.1	34	8.2–12.4	180
CNT/UHMWPE	4 wt%	2	30.1	32.6	8–18	181
PLA/Ag	5.89 vol%	1.5	254	50	8.2–12.4	182
PVDF/MWNT	7 wt%	3	6	45	8.2–12.4	183
PLLA/MWNT	1.1 wt%	1.5	25	30	8.2–12.4	184

other structure-based strategies. Typically, two approaches are employed for developing segregated structures. One approach is the addition of conductive fillers to form a percolated network in the polymer matrix through the densification process. The conductive filler loadings in the segregated network structure resulted in a percolated conductive network structure integrated with the polymer matrix. Furthermore, the segregation of conductive fillers by distinct polymeric bulks improves the composite's EMI shielding performance. The other approach is to prefabricate 3D integrated conductive structures, and subsequently fill the pores with the polymer matrix (Fig. 12).

Li et al. presented a novel process for producing a segregated composite of poly(phenylene sulfide) (PPS) containing carbon nanotubes (CNT).[174] Firstly, PPS beads were mechanically blended with CNT to produce PPS complex granules coated with CNT. This was followed by compression molding into segregated composites of CNT/PPS. The EMI shielding effectiveness of the segregated composite of CNT/PPS was significantly higher than that of the random ones. Segregated structures exhibited excellent EMI shielding effectiveness.[174] Similarly, Sun et al. studied an electrostatic assembly method for producing highly conductive polystyrene (PS) nanocomposites containing MXene.[175] In this method, the pre-coating of negative MXene on positive PS microspheres was followed by compression molding. The resulting PS composites containing MXene have a lower percolation threshold limit of 0.26 vol%,

resulting in a good electrical conductivity of 1081 S m^{-1} and an excellent EMI SE of 54 dB over the X-band frequency range of 8–12.4 GHz.[175] Liang et al. developed a three-dimensional foam with systematic hollow spherical structures of reduced graphene oxide and silver platelets (rGO/AgP).[161] By using a freeze-drying process, the foam composite accomplished a uniform distribution of AgP and rGO, forming a network structure. The final nanocomposites containing highly stable segregated structures were successfully fabricated by backfilling the epoxy monomer and curing agent. The 3D segregated structures of AgP/rGO/EP nanocomposites containing 0.44 vol% rGO and 0.94 vol% AgP showed the maximum SE$_T$ value of 58 dB in the X-band frequency range of 8–12.4 GHz and electrical conductivity of 45.3 S m^{-1} due to systematic percolation networks of the AgP/rGO hollow spherical particles and the interfacial synergy between hollow spherical particles and epoxy resin.[161] Many authors have reported segregated structures in the literature that are used in the fabrication of EMI shielding materials which are listed in Table 9.

3.9 Template structure

In the polymer composites, the addition of large filler loadings of nanomaterials in the polymer matrix attenuates EM waves. The addition of large filler loadings in the polymer matrix resulted in the formation of agglomerates and the dense
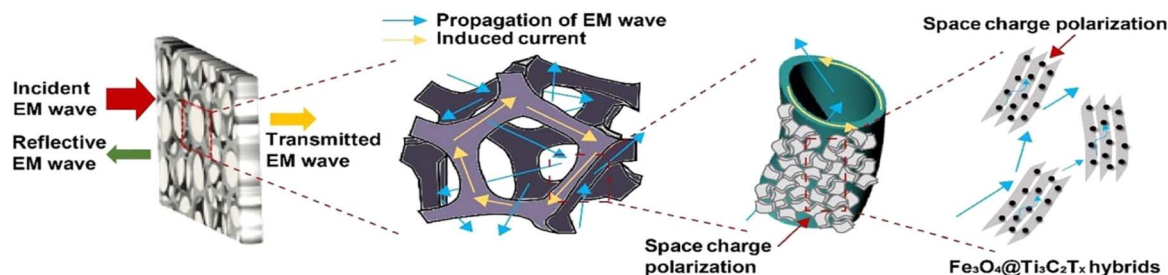

Fig. 13 Schematic diagram of the EM waves absorption in the Fe$_3$O$_4$@Ti$_3$C$_2$T$_x$/GF/PDMS composite. Reprinted with permission. Copyright (2020).[186]

Table 10 The template-based structures for the fabrication of EMI shielding materials

Materials	Template	Conductivity (S m^{-1})	SE$_T$ (dB)	Frequency (GHz)	Ref.
10.69 wt% MXene (Ti$_3$C$_2$T$_x$)/PDMS			30	8.2–12.4	186
10.69 wt% Graphene/PDMS			15	8.2–12.4	186
10.69 wt% MXene/11.53 wt% Fe$_3$O$_4$/graphene/PDMS	Graphene		80	8.2–12.4	186
10.69 wt% MXene/11.53 wt% Fe$_3$O$_4$/graphene/PDMS	Graphene		77	26.5–40	186
1.2 wt% rGO/MXene/epoxy	Al$_2$O$_3$	36	43.5	8.2–12.4	188
3.3 wt% rGO/MXene/epoxy	Al$_2$O$_3$	387.1	55	8.2–12.4	188
12 wt% Graphene foam/hollow-Fe3O$_4$/polydimethylsiloxane	Nickel foam		70.37	8.2–12.4	189
2.76 wt% Fe$_3$O$_4$ chemically bonded carbon nanotubes/reduced graphene foams (RGF)/epoxy	RGF	7.3×10^{-5}	36	8.2–12.4	190
2.76 wt% carbon nanotubes/reduced graphene foams/epoxy	RGF	14	31	8.2–12.4	190
2.58 wt% PANI/0.83 wt% MWCNT/1.20 wt% thermally annealed graphene/epoxy	PANI	5210	42	8.2–12.4	191
1.5 wt% Fe$_3$O$_4$/1.2 wt% thermally annealed graphene oxide/epoxy	Graphene	8.7×10^{-5}	10	8.2–12.4	192
1.5 wt% Fe$_3$O$_4$/1.2 wt% thermally annealed graphene/epoxy	Graphene	27.5	35	8.2–12.4	192

stacking of polymers in the nanocomposite. In response to such problems, introducing 3D porous template structures will effectively overcome the agglomeration of nanomaterials. There were major studies on template-based polymer composites and the researchers used templates to create 3D porous structures. Song et al. used a sacrificial template approach to build 3D foam structures with rGO and MXene.[185] The template was produced from an Al$_2$O$_3$ honeycomb plate. MXene self-assembly on rGH resulted in honeycomb structural rGO-MXene (rGMH) with the formation of percolated networks and excellent EMI shielding properties. The honeycomb cell size of 0.5 mm contains 1.2 wt% rGO and 3.3 wt% MXene/epoxy nanocomposite demonstrating the electrical conductivity of 387.1 S m^{-1} and SE$_T$ value of 55 dB values[185] (Fig. 13).

Recently, Shahzad et al. who studied renewable porous biochar and 2D MXene have sparked tremendous interest in high-performance EMI shielding fields due to their particular ordered structures and good electrical conductivity values.[187] The wood-based porous carbon from natural wood was used as a template in this study. The composites containing 15 wt% MXene/epoxy and 4.25 wt% MXene foam/epoxy were prepared by direct blending and template methods corresponding to SE$_T$ values of 41 and 46 dB, respectively. Many authors have reported template-based structures in the literature for the fabrication of EMI shielding materials which are listed in Table 10.

4 Process-based strategies of nanomaterials for the fabrication of efficient EMI shielding materials

To develop EMI shielding materials, the homogeneous distribution of nanomaterials in the polymeric matrix is

a fundamental design strategy focused on delivering uniform dispersion of the incorporated fillers in the polymer. The nanomaterials in the polymer matrix combined to create a percolation network that relies on a filler loading of nanoparticles. Nevertheless, nanofillers have various sizes and multiple dimensions, and the filler loading of nanoparticles in large quantities makes them vulnerable to agglomeration in the polymer matrix, thereby significantly affecting the composites' performances.[4] The miscibility of nanoparticles may increase by introducing an external force. Melt blending, solvent mixing, and in situ polymerization are all approaches for achieving a homogeneous structure. Melt blending is an economically feasible, cost-effective, and realistic method in the polymer industry. In this method, the polymer matrix was heated at melting temperature rather than its solubility in conventional solvents, preventing the solvent removal stage.[4]

The high-quality shear mixing method will ensure that the fillers are well dispersed in the molten polymer. Kumar et al. used a continuous melt blending technique to achieve homogeneous dispersion of large filler loadings of MWNT within a polypropylene (PP) polymeric matrix.[11] Morphological characteristics were analysed and confirm the good dispersion of MWNT in the nanocomposites. The nanocomposite with an MWNT loading of 2 wt% demonstrated an SE$_T$ value of 5.9 dB, which corresponds to 74.29% attenuation of incident EM wave power over the X-band frequency range of 8–12.4 GHz. Many authors have reported in the literature the melt blending method used in the fabrication of EMI shielding materials listed in Table 10.

Solution mixing depends on a solvent technique, which finely disperses the fillers in the matrix due to the polymer's lower viscosity. Because of the filler's limited solubility in the solvent, certain processing steps such as intense stirring, high-

Table 11 Processing strategies used in the fabrication of efficient EMI shielding materials

Materials	Method	Conductivity (S m^{-1})	SE$_T$ (dB)	Frequency (GHz)	Ref.
Fabrics/10 wt% CNT and sodium alginate	20 Cycles of layer-by-layer assembly	36.6	21.5	8.2–12.4	195
Fabrics/10 wt% CNT and sodium alginate	20 Cycles of layer-by-layer assembly	36.6	20.8	12.4–18	195
PS/5 wt% MWCNT	Nano-infiltration	7.2×10^{-2}	25	8.2–12.4	196
PS/5 wt% MWCNT/rGO/Fe$_3$O$_4$	Nano-infiltration	0.014	22	8.2–12.4	196
PS/5 wt% MWCNT/rGO/MoS$_2$	Nano-infiltration	0.031	36	8.2–12.4	196
PLA/30 wt% PVDF/0.25 wt% CNT	Kinetically controlled melt blending	1.06×10^{-2}	<3.5	8.2–12.4	197
PLA/30 wt% PVDF/0.25 wt% CNT	Kinetically controlled melt blending	1.06×10^{-2}	<8	1–6	197
20 vol% PS/PMMA/2.7 vol% MWNT	Intertube and interphase controlled melt blending	90	29–20	8.2–12.4	198
PDMS/3 wt% MWNT	Spin coating	40	13.5	8.2–12.4	199
PDMS/3 wt% MWNT	Compression molding	88	7	8.2–12.4	199
50 wt% PC/PMMA/3 wt% MWNT	Solution mixing	0.5	8–14	8–12	200
50 wt% PC/PMMA/3 wt% MWNT	Melt blending	0.3	4.5–9	8–12	200
0.5 wt% E-f-GO/epoxy/carbon fiber	VARTM technique	—	55–67	12.4–18	201
PVDF/30 wt% Ni	The rotational orientation of filler	—	20–35	26.5–40	202
7.5 wt% (graphene/MWNT)/PBO	In situ polymerization		50.17	12.58	203
2 wt% Ionic liquid-MWNT + 5 wt% BaFe in PC + 10 wt% PMMA	Melt blending	2.8	37	8–18	204
PET/PANI composite	In situ chemical oxidation polymerization method	80	23.95	8–12.4	205
35 wt% EVA/40 wt% CF/5 wt% OMMT/20 wt% SCF	Ceramization	99	36	8–12.4	206
PS/12.6 vol% Cu	Compression molding	2.95×10^6	100	0.1–18	207
PS/12.6 vol% Cu/0.4 vol% Ag	Compression molding	3.5×10^6	110	0.1–18	207
PVDF/2 wt% MWNT	Extrusion followed rolling	2.8×10^{-3}	18–25	12–18	208
EMA/50 wt% EOC/15 wt% MWNT	Solution mixing	0.89	33	8–12.4	209
60 wt% AEM/MPU/5 wt% SWNT	Blending	4.27×10^{-2}	23–27	2–8	210
ABS/1.5 wt% CNT/1.5 wt% CB	Extrusion followed by vacuum drying	4.7×10^{-3}	11	8–12.4	211
ABS/3 wt% CNT	Extrusion followed by vacuum drying	1.27×10^{-3}	17	8–12.4	211
40 wt% CNT/PLA	Melt blending	3.2	50	8–12.4	212
40 wt% CNT/PLA	3D printing	1.1	30	8–12.4	212
48 wt% poly(ʟ-lactide)/12 wt% poly(ε-caprolactone)/PCL/2 carbon nanotubes	Melt blending	0.012	17	8–12.4	213

intensity ultrasonication, and surface modification are needed. Ouyang *et al.* produced an intrinsically conducting polymer composed of poly(3,4-ethylene dioxythiophene) (PEDOT) and polystyrene sulfonate (PSS) as a conductive portion for the development of highly effective flexible EMI materials.[193] PEDOT and PSS were mixed with an extremely stretchable, miscible polyurethane (PU) solution to create composite films by drop-casting. The 0.15 mm thick films exhibited a conductivity of 7.7×10^3 S m^{-1} and demonstrated a SE$_T$ value of 62 dB over the X-band frequency range of 8–12.4 GHz. *In situ* polymerization is a reasonably complex process in which the dispersion of the filler is timed to correspond with the matrix's polymerization. Zhang *et al.* generated a sequence of conductive polymeric composites by polymerizing an ε-caprolactam monomer *in situ* in the presence of GO nanosheets in a single step.[194] The reduction, refinement, and distribution of GOs occurred by polymerization, with no additional reducing agents utilized. In the *in situ* polymerization process, epoxy-based composites were commonly used. The addition of the nanoparticles in the composite helped create conductive networks while also contributing to hysteresis degradation, resulting in significantly enhanced absorption of EM waves. It is believed that by using various processes, a more efficient polymer composite containing filler loading of nanoparticles would be possible, which would be accomplished using processing techniques as listed in Table 11.

5 Sustainable strategies of nanomaterials for the fabrication of efficient EMI shielding materials

A sustainable polymer is a plastic material that satisfies consumer demands without harming the environment, health, or economy. To accomplish this, scientists are focusing on creating polymers that, as compared to non-sustainable alternatives, use renewable feedstocks, such as plants and crops for manufacturing with a smaller carbon footprint and a facile end life. Although sustainable polymers are a significant rising segment of the industry, they are derived from unsustainable fossil materials and require adequate synthesis and processing. A natural polymer, as a non-toxic, reusable, and renewable fuel, may be directly carbonized to produce macroscopic materials without the use of expensive precursors or complicated processes, implying an efficient energy-saving path for EMI shielding materials. As precursors, two prominent natural products, cellulose and lignin, have received considerable attention. Since graphene oxide can only be uniformly
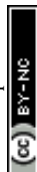
Table 12 Sustainable nanocomposites used in EMI shielding applications

Materials	Novelty	Filler content	Thickness (mm)	Conductivity (S m^{-1})	EMI SE (dB)	Frequency (GHz)	Ref.
PU/MWCNTs/Fe$_3$O$_4$@MoS$_2$	Self-healing composites	3 wt% MWCNT; 5 wt% Fe$_3$O$_4$@MoS$_2$	5	—	−36.6	8–18	218
MWCNTs/rGO/Fe$_3$O$_4$/PU	Ultrafast self-healing composites	3 wt% MWCNT; 5 wt% rGO/Fe$_3$O$_4$	5.8	0.05	−36	8–18	219
PU/MWCNTs/ rGO@MoS$_2$@Fe$_3$O$_4$	Trigger free self-healing	3 wt% MWCNT; 5 wt% rGO@MoS$_2$@Fe$_3$O4	5	10^{-1}	−43.6	8–18	220
GEs/CNTs/Elastomeric ionomers	Recyclable and self-healing (100% recovery)	10 wt%	1	550	64	8.2–12.4	221
Fe$_3$O$_4$@MWCNTs/PAM	Recoverable and self-healing	20 wt% Fe$_3$O$_4$@MWCNTs	1.8	—	−50	8.2–12.4	222
MWCNT/Ni@CLF/PEEK	Renewable biomaterials	18 wt% Ni@CLF	2.5	2.101	48.1	8.2–12.4	223
PLLA/CPEGDA/MWCNT	Sustainable eco-friendly	3.6 vol% MWCNT	1	10^{-1}	27.4	8.2–12.4	224
PLA/GNP	Naturally derived biodegradable nanocomposites	15 wt% GNP	2.5	7.4	15	8.2–12.4	225
PBAT/GNP	Naturally derived biodegradable nanocomposites	15 wt% GNP	2.5	3	14	8.2–12.4	225
PLA/Graphite foams	Renewable and biodegradable nanocomposites	2.5 wt%	2	3.5	45	8.2–12.4	226
PLA/Graphite solid	Renewable and biodegradable nanocomposites	2.5 wt%	2	2×10^{-6}	20	8.2–12.4	226
PLA/MWCNT foams	Biodegradable nanocomposites	0.0054 vol% MWCNT	5	—	45	8.2–12.4	227
PLA/GNP	Biodegradable nanocomposites	15 wt% GNP	1.5	7.4	15.5	5.85–12.4	228
PLLA-MWCNT	Biodegradable nanocomposites	10 wt% MWCNT	2.5	3.4	23	8.2–12.48	229
PANI/CNF	Environment friendly and sustainable	50 wt% PANI and 50 wt% CNF	1	31.4	−23	8.2–12.4	230
Waste paper/Ag-based ink	Waste paper based composite	—	0.36	—	68	10.77–18	231
WTP/PVA carbon aerogel	Waste tissue paper based carbon absorbing composite	6 wt% Waste tissue paper	—	135	40	8.2–12.4	232
PVB-CoO$_x$-FAC	Usage of waste fly ash cenospheres	10 wt%	2.5	—	−27	15.8	233
PVB-NiO-FAC	Usage of waste fly ash cenospheres	10 wt%	2.5	—	−47.5	15.8	233
PVB-PANI-FAC	Usage of waste fly ash cenospheres	10 vol% FAC; 30 vol% PANI; 60 vol% PVB	265 ± 2 μm	11	15	5.8–12.4	234
PVB-PANI-Ni-FAC	Usage of waste fly ash cenospheres	10 vol% Ni-FAC; 30 vol% PANI; 60 vol% PVB	259 ± 2 μm	18 S m^{-1}	23 ± 1	5.8–12.4	234
PVB-PANI-Co-FAC	Usage of waste fly ash cenospheres	10 vol% Co-FAC; 30 vol% PANI; 60 vol% PVB	261 ± 2 μm	21 S m^{-1}	19	5.8–12.4	234
BC/Cu/Al$_2$O$_3$	Usage of bacterial cellulose	—	—	0.69×10^{-12} S m^{-1}	65.3	1.5	235
PP/rGO	Usage of vitamin C for in situ reduction of rGO	20 wt% rGO	2	10^{-1} S m^{-1}	50	8–18	236

distributed in water at lower concentrations, the resulting graphene aerogels have low density, good mechanical strength, and conductivity. In contrast to graphene oxide, Zeng *et al.* discovered that lignin could form stable suspensions in a much wider range of concentrations, resulting in honeycomb-like foams with tunable densities through unidirectional freeze-drying.[214] As a result of their research, honeycomb-like lignin-derived carbon (LC) foams doped with rGO were created using unidirectional ice-templating, freeze-drying, and carbonization. The interfaces between the LC and rGO and the aligned pores in the 2 mm thick honeycomb-like foams contributed interfacial polarization loss and numerous reflections, resulting in a collection of 31 dB over the X-band frequency range of 8–12.4 GHz. Because of their broad specific area and porous nature, Wan *et al.* chose cellulose-derived carbon aerogels (CDCA) as materials.[215] Then, using a simple chemical precipitation process, nanoneedles and nanoflowers of magnetic α-FeOOH were developed *in situ* on a CDCA substrate to increase the contributions of magnetic losses and thus improve the EMI shielding characteristics. The incorporation of α-FeOOH into carbon aerogels exhibited an absorption-dominant mechanism, which certainly reduced secondary radiation from EMI shields as a prepared composite was a compelling option for designing safety devices from EM radiation. Furthermore, a volume of natural biomass rich in natural polymers, such as wood, straw, pulp, flour, cotton, and sugarcane, has been used as a precursor, which has proven to be a potential candidate for application as an EMI shielding material. Another area of importance should be recovering materials from electrical and electronic devices into the matrix and reinforcement for EMI shielding applications leading to waste management and sustainability. Rosa *et al.* worked on using e-waste as metal fillers to the polymer matrix. The polymer matrix was high density polyethylene (HDPE) recovered from municipal solid waste. The metal filler, mostly iron oxide, was separated from printed circuit boards (PCB), and the EMI SE was observed to be 48.3 dB. Rahaman *et al.* investigated recycling and reusing polyethylene (PE) from waste plastic materials to be used as a packaging material for electronic devices. Carbon black was used as the conducting filler to improve the shielding properties, and the composite showed an EMI SE value of 33 dB at a thickness of 1 mm and an attenuation of 99.93%.[216,217] Many authors have reported sustainable nanocomposites for EMI shielding purposes which are listed in Table 12.

6 Summary and perspective

Electromagnetic interference (EMI) has evolved as a result of rapid advances in the sectors of electronics and communications, offering a great opportunity for the development of efficient EMI shielding materials. Owing to continuous exploratory efforts, polymer composites comprising conductive, magnetic, and/or dielectric materials as important constituents for preventing electromagnetic interference (EMI) are reported. Several processing techniques for the preparation of EMI shielding materials were discussed in this review. The structural design of nanofillers is critical and challenging work in the fabrication of EMI shielding

materials, which integrates the functional filler with the polymer matrix for superior EMI shielding performance. Firstly, the role of the basic nanofiller in the preparation of high-performance EMI shielding composites was outlined, along with preparation techniques and typical cases. Also, different-structured nanofillers used simultaneously during the fabrication process to improve shielding performance were discussed. Secondly, the importance of the fabrication process for developing EMI shielding materials was summarized. In addition, different manufacturing strategies for lightweight and ultra-thin materials were addressed in order to be used as potential EMI shielding materials. Synthetic and natural polymers have been processed into various derivatives using facile synthesis processes that demonstrate significant promise for adequate preparations of EMI shielding materials. Furthermore, simple, large-scale, and low-cost fabrication methods for EMI shielding materials for efficient industrialization and emerging structures were explored, as should the translation of corresponding shielding devices for potential applications. Finally, EMI shielding material fabrication techniques endow the EMI shields with unique properties, transforming them into high-value-added EMI shielding materials.

Nomenclature

ABS	Acrylonitrile-butadiene-styrene
AEM	Ethylene acrylic elastomers
AIBN	Azoisobutyronitrile
Ag	Silver nanoparticles
Ag@HGM	Silver nanoparticles on the surface of hollow glass microspheres
BC	Bacterial cellulose
BN	Boron nitride
BNSF	$BaNd_{0.2}Sm_{0.2}Fe_{11.6}O_{19}$
BRF	Polypyrrole matrix encapsulated with BST, RGO and Fe_3O_4
BST	Barium strontium titanate
CB	Carbon black
CCTO	$CaCu_3Ti_4O_{12}$
CDCA	Cellulose-derived carbon aerogels
CF	Carbon fibre
CLF	Carbonized loofah fiber
CNF	Cellulose nanofiber
CNT	Carbon nanotubes
CPEGDA	Crosslinked poly(ethylene glycol) diacrylate
CSA	Camphor sulfonic acid
EM	Electro-magnetic
EMA	Ethylene-*co*-methyl acrylate
EMI	Electro-magnetic interference
EMI SE	Electro-magnetic interference shielding effectiveness
EOC	Ethylene octene copolymer
FAC	Fly ash cenosphere
f-MWCNT	Functionalized multiwalled carbon nanotubes
GFBT	Graphene nanoplate/Fe_3O_4@$BaTiO_3$ hybrid
GN	Graphene nanosheets
GN-CN	Graphene nanoplates-carbon nanotubes
GNP	Graphene nanoplatelets

HDPE	High density polyethylene
HGM	Hollow glass microspheres
IL-MWCNT	Ionic liquid-multiwalled carbon nanotubes
Lbl	Layer-by-layer
LC	Lignin-derived carbon
MA	Maleic anhydride
MNP	Metal nanoparticles
MPU	Millable polyurethane
MWNT or MWCNT	Multi-walled carbon nanotubes
NCF	Nickel doped cobalt ferrites
NF	Nonwoven fabric
Ni@CNT	Carbon nanotube encapsulated nickel nanowires
NR	Natural rubber
NWF	Non-woven fabrics
PAM	Polyazomethine
PANI	Polyaniline
PBAT	Poly(butylene adipate-co-terephthalate)
PBO	Poly(p-phenylene benzobisoxazole)
PC	Polycarbonate
PCL	Polycaprolactone
PDMS	Polydimethylsiloxane
PEDOT	Poly(3,4-ethylene dioxythiophene)
PEEK	Polyether ether ketone
PET	Polyethylene terephthalate
PET oxide	Poly(ethylene oxide)
PHDDT	Phosphorus-containing liquid crystalline co-polyester
P_I	Power density of incident electromagnetic waves
PLA	Poly(lactic acid)
PLLA	Poly(L-lactide)
PMMA	Poly(methyl methacrylate)
PNC	Polymer nanocomposites
POE	Poly(ethylene-co-1-octene)
PP	Polypropylene
PPy	Polypyrrole
PPEK	Poly(phthalazinone ether ketone)
PPS	Poly(phenylene sulphide)
P_R	Power density of reflected electromagnetic waves
PS	Polystyrene
PSS	Polystyrene sulfonate
P_T	Power density of transmitted electromagnetic waves
p-TSA	para-Toluene sulphonic acid
PVA	Polyvinyl alcohol
PVB	Poly(vinyl butyral)
PVDF	Polyvinylidene fluoride
RG-CN	Chemically reduced graphene oxide-carbon nanotubes
rGH	Honeycomb structural rGO
rGMH	Honeycomb structural rGO-MXene
RGO	Reduced graphene oxide
SBR	Styrene-butadiene rubber
SCF	Short carbon fiber
SE_A	EMI shielding effectiveness due to absorption loss

SE_R	EMI shielding effectiveness due to reflection loss
SE_T	Total EMI shielding effectiveness
SGM	Solid glass microspheres
SSE	Specific shielding effectiveness
SSF	Stainless steel fibre
Sub-SF	Substituted strontium ferrite
SWNT	Single-walled carbon nanotube
TAGA	Thermally annealed graphene aerogel
TGO	Thermally reduced graphene oxide
TGO-CN	Thermally reduced graphene oxide-carbon nanotubes
TPU	Thermoplastic polyurethane
UHMWPE	Ultrahigh-molecular-weight polyethylene
WPU	Waterborne polyurethane
WTP	Wastepaper

Data availability

No primary research results, software or code have been included and no new data were generated or analysed as part of this review.

Conflicts of interest

All authors declare that they have no conflicts of interest.

References

1 S. Sankaran, K. Deshmukh, M. B. Ahamed and S. K. Khadheer Pasha, Recent advances in electromagnetic interference shielding properties of metal and carbon filler reinforced flexible polymer composites: A review, *Composites, Part A*, 2018, **114**, 49–71, DOI: 10.1016/j.compositesa.2018.08.006.

2 X. C. Tong, *Advanced materials and design for electromagnetic interference shielding text book*, 2009.

3 C. R. Paul, *Introduction to Electromagnetic Compatibility*, Wiley Series in Microwave and Optical Engineering, 2nd edn, 2006.

4 K. Bhaskaran, R. K. Bheema and K. C. Etika, The influence of Fe₃O₄@GNP hybrids on enhancing the EMI shielding effectiveness of epoxy composites in the X-band, *Synth. Met.*, 2020, **265**, 116374, DOI: 10.1016/j.synthmet.2020.116374.

5 V. Uma Varun, B. Rajesh Kumar and K. C. Etika, Hybrid polymer nanocomposites as EMI shielding materials in the X-band, *Mater. Today: Proc.*, 2019, **28**, 796–798, DOI: 10.1016/j.matpr.2019.12.300.

6 B. Rajesh Kumar and K. C. Etika, Facile One-Pot Hydrothermal Synthesis of Copper Nanowires and Their Impact on the EMI Shielding Capability of Epoxy Composites, *Chem. Eng. Technol.*, 2022, **45**(3), 410–416, DOI: 10.1002/ceat.202100389.

7 R. K. Bheema, A. K. Ojha, A. V. Praveen Kumar and K. C. Etika, Synergistic influence of barium hexaferrite nanoparticles for enhancing the EMI shielding

performance of GNP/epoxy nanocomposites, *J. Mater. Sci.*, 2022, **57**(19), 8714–8726, DOI: 10.1007/s10853-022-07214-8.

8 S. Liu, S. Qin, Y. Jiang, P. Song and H. Wang, Lightweight high-performance carbon-polymer nanocomposites for electromagnetic interference shielding, *Composites, Part A*, 2021, **145**, 106376, DOI: 10.1016/j.compositesa.2021.106376.

9 A. K. Singh, A. Shishkin, T. Koppel and N. Gupta, A review of porous lightweight composite materials for electromagnetic interference shielding, *Composites, Part B*, 2018, **149**, 188–197, DOI: 10.1016/j.compositesb.2018.05.027.

10 L. Wang, Z. Ma, Y. Zhang, L. Chen, D. Cao and J. Gu, Polymer-based EMI shielding composites with 3D conductive networks: A mini-review, *SusMat*, 2021, **1**(3), 413–431, DOI: 10.1002/sus2.21.

11 R. Kumar, K. Kumar, N. Etakula and K. C. Etika, Enhanced thermo-mechanical , thermal and EMI shielding properties of MWNT/MAgPP/PP nanocomposites prepared by extrusion, *Compos., Part C: Open Access*, 2021, **4**, 100086, DOI: 10.1016/j.jcomc.2020.100086.

12 R. Turczyn, K. Krukiewicz, A. Katunin, J. Sroka and P. Sul, Fabrication and application of electrically conducting composites for electromagnetic interference shielding of remotely piloted aircraft systems, *Compos. Struct.*, 2020, **232**, 111498, DOI: 10.1016/j.compstruct.2019.111498.

13 H. K. Choudhary, R. Kumar, S. P. Pawar, S. Bose and B. Sahoo, Effect of Microstructure and Magnetic Properties of Ba-Pb-Hexaferrite Particles on EMI Shielding Behavior of Ba-Pb-Hexaferrite-Polyaniline-Wax Nanocomposites, *J. Electron. Mater.*, 2020, **49**(3), 1618–1629, DOI: 10.1007/s11664-019-07478-y.

14 B. Zhang, J. Wang, J. Wang, H. Duan, S. Huo and Y. Tang, Coprecipitation synthesis of hollow poly(acrylonitrile) microspheres@CoFe$_2$O$_4$ with graphene as lightweight microwave absorber, *J. Mater. Sci.: Mater. Electron.*, 2017, **28**(4), 3337–3348, DOI: 10.1007/s10854-016-5927-x.

15 T. Su, B. Zhao, F. Han, B. Fan and R. Zhang, The effect of hydrothermal temperature on the crystallographic phase of MnO2 and their microwave absorption properties, *J. Mater. Sci.: Mater. Electron.*, 2019, **30**(1), 475–484, DOI: 10.1007/s10854-018-0312-6.

16 B. Zhang, *et al.*, Double-shell PANS@PANI@Ag hollow microspheres and graphene dispersed in epoxy with enhanced microwave absorption, *J. Mater. Sci.: Mater. Electron.*, 2019, **30**(10), 9785–9797, DOI: 10.1007/s10854-019-01315-y.

17 M. K. Naidu, K. Ramji, B. V. S. R. N. Santhosi, K. Krushna Murthy, C. Subrahmanyam and B. Satyanarayana, Influence of NiFe Alloy Nanopowder on Electromagnetic and Microwave Absorption Properties of MWCNT/Epoxy Composite, *Adv. Polym. Technol.*, 2018, **37**(2), 622–628, DOI: 10.1002/adv.21703.

18 M. K. Vyas and A. Chandra, Synergistic effect of conducting and insulating fillers in polymer nanocomposite films for attenuation of X-band, *J. Mater. Sci.*, 2019, **54**(2), 1304–1325, DOI: 10.1007/s10853-018-2894-z.

19 L. Liu, *et al.*, Electromagnetic response of magnetic graphene hybrid fillers and their evolutionary behaviors, *J. Mater. Sci.: Mater. Electron.*, 2016, **27**(3), 2760–2772, DOI: 10.1007/s10854-015-4088-7.

20 X. S. Hu, Y. Shen, L. S. Lu, J. Xu and J. J. Zhen, Enhanced electromagnetic interference shielding effectiveness of ternary PANI/CuS/RGO composites, *J. Mater. Sci.: Mater. Electron.*, 2017, **28**(9), 6865–6872, DOI: 10.1007/s10854-017-6386-8.

21 H. Lu, *et al.*, Electromagnetic shielding of ultrathin, lightweight and strong nonwoven composites decorated by a bandage-style interlaced layer electropolymerized with polyaniline, *J. Mater. Sci.: Mater. Electron.*, 2019, **30**(23), 20420–20431, DOI: 10.1007/s10854-019-02379-6.

22 G. Sun, H. Wu, Q. Liao and Y. Zhang, Enhanced microwave absorption performance of highly dispersed CoNi nanostructures arrayed on graphene, *Nano Res.*, 2018, **11**(5), 2689–2704, DOI: 10.1007/s12274-017-1899-2.

23 M. P. Gashti, S. T. Ghehi, S. V. Arekhloo, A. Mirsmaeeli and A. Kiumarsi, Electromagnetic shielding response of UV-induced polypyrrole/silver coated wool, *Fibers Polym.*, 2015, **16**(3), 585–592, DOI: 10.1007/s12221-015-0585-9.

24 D. Jiang, *et al.*, Electromagnetic Interference Shielding Polymers and Nanocomposites – A Review, *Polym. Rev.*, 2019, **59**(2), 280–337, DOI: 10.1080/15583724.2018.1546737.

25 K. Müller, *et al.*, Microwave Absorption and EMI Shielding Behavior of Nanocomposites Based on Intrinsically Conducting Polymers, Graphene and Carbon Nanotubes, *Carbon*, 2014, **4**(1), 371–375, DOI: 10.5772/48779.

26 N. Maruthi, M. Faisal and N. Raghavendra, Conducting polymer based composites as efficient EMI shielding materials: A comprehensive review and future prospects, *Synth. Met.*, 2021, **272**, 116664, DOI: 10.1016/j.synthmet.2020.116664.

27 M. Z. Rong, M. Q. Zhang, Y. X. Zheng, H. M. Zeng, R. Walter and K. Friedrich, Structure-property relationships of irradiation grafted nano-inorganic particle filled polypropylene composites, *Polymer*, 2001, **42**(1), 167–183, DOI: 10.1016/S0032-3861(00)00325-6.

28 F. P. Du, *et al.*, PEDOT:PSS/graphene quantum dots films with enhanced thermoelectric properties *via* strong interfacial interaction and phase separation, *Sci. Rep.*, 2018, **8**(1), 1–12, DOI: 10.1038/s41598-018-24632-4.

29 J. B. Hooper and K. S. Schweizer, Theory of phase separation in polymer nanocomposites, *Macromolecules*, 2006, **39**(15), 5133–5142, DOI: 10.1021/ma060577m.

30 H. Xia and M. Song, Preparation and characterization of polyurethane-carbon nanotube composites, *Soft Matter*, 2005, **1**(5), 386–394, DOI: 10.1039/b509038e.

31 Z. Zeng, H. Jin, M. Chen, W. Li, L. Zhou and Z. Zhang, Lightweight and Anisotropic Porous MWCNT/WPU Composites for Ultrahigh Performance Electromagnetic Interference Shielding, *Adv. Funct. Mater.*, 2016, **26**(2), 303–310, DOI: 10.1002/adfm.201503579.

32 Y. Zhang, T. Pan and Z. Yang, Flexible polyethylene terephthalate/polyaniline composite paper with bending durability and effective electromagnetic shielding

performance, *Chem. Eng. J.*, 2020, **389**, 124433, DOI: 10.1016/j.cej.2020.124433.

33 K. Bhaskaran, R. K. Bheema, K. C. Etika, B. Krithika, B. R. Kumar and K. C. Etika, The influence of Fe$_3$O$_4$@GNP hybrids on enhancing the EMI shielding effectiveness of epoxy composites in the X-band, *Synth. Met.*, 2020, **265**, 116374, DOI: 10.1016/j.synthmet.2020.116374.

34 Y. Liu, D. Song, C. Wu and J. Leng, EMI shielding performance of nanocomposites with MWCNTs, nanosized Fe$_3$O$_4$ and Fe, *Composites, Part B*, 2014, **63**, 34–40, DOI: 10.1016/j.compositesb.2014.03.014.

35 H. Jia, *et al.*, 3D graphene/carbon nanotubes/polydimethylsiloxane composites as high-performance electromagnetic shielding material in X-band, *Composites, Part A*, 2020, **129**, 105712, DOI: 10.1016/j.compositesa.2019.105712.

36 K. Yu, *et al.*, RGO/Fe$_3$O$_4$ hybrid induced ultra-efficient EMI shielding performance of phenolic-based carbon foam, *RSC Adv.*, 2019, **9**(36), 20643–20651, DOI: 10.1039/c9ra04244j.

37 N. Bagotia, V. Choudhary and D. K. Sharma, Synergistic effect of graphene/multiwalled carbon nanotube hybrid fillers on mechanical, electrical and EMI shielding properties of polycarbonate/ethylene methyl acrylate nanocomposites, *Composites, Part B*, 2019, **159**, 378–388, DOI: 10.1016/j.compositesb.2018.10.009.

38 H. Liu, *et al.*, Novel 3D network porous graphene nanoplatelets/Fe$_3$O$_4$/epoxy nanocomposites with enhanced electromagnetic interference shielding efficiency, *Compos. Sci. Technol.*, 2019, **169**, 103–109, DOI: 10.1016/j.compscitech.2018.11.005.

39 J. Chen, J. Wu, H. Ge, D. Zhao, C. Liu and X. Hong, Reduced graphene oxide deposited carbon fiber reinforced polymer composites for electromagnetic interference shielding, *Composites, Part A*, 2016, **82**, 141–150, DOI: 10.1016/j.compositesa.2015.12.008.

40 M. Verma, S. S. Chauhan, S. K. Dhawan and V. Choudhary, Graphene nanoplatelets/carbon nanotubes/polyurethane composites as efficient shield against electromagnetic polluting radiations, *Composites, Part B*, 2017, **120**, 118–127, DOI: 10.1016/j.compositesb.2017.03.068.

41 S. K. Singh, M. J. Akhtar and K. K. Kar, Hierarchical Carbon Nanotube-Coated Carbon Fiber: Ultra Lightweight, Thin, and Highly Efficient Microwave Absorber, *ACS Appl. Mater. Interfaces*, 2018, **10**(29), 24816–24828, DOI: 10.1021/acsami.8b06673.

42 C. Liu, X. Ye, X. Wang, X. Liao, X. Huang and B. Shi, Collagen Fiber Membrane as an Absorptive Substrate to Coat with Carbon Nanotubes-Encapsulated Metal Nanoparticles for Lightweight, Wearable, and Absorption-Dominated Shielding Membrane, *Ind. Eng. Chem. Res.*, 2017, **56**(30), 8553–8562, DOI: 10.1021/acs.iecr.7b01930.

43 S. Shajari, M. Arjmand, S. P. Pawar, U. Sundararaj and L. J. Sudak, Synergistic effect of hybrid stainless steel fiber and carbon nanotube on mechanical properties and electromagnetic interference shielding of polypropylene nanocomposites, *Composites, Part B*, 2019, **165**, 662–670, DOI: 10.1016/j.compositesb.2019.02.044.

44 A. H. A. Hoseini, M. Arjmand, U. Sundararaj and M. Trifkovic, Significance of interfacial interaction and agglomerates on electrical properties of polymer-carbon nanotube nanocomposites, *Mater. Des.*, 2017, **125**, 126–134, DOI: 10.1016/j.matdes.2017.04.004.

45 P. Saini, V. Choudhary, B. P. Singh, R. B. Mathur and S. K. Dhawan, Polyaniline-MWCNT nanocomposites for microwave absorption and EMI shielding, *Mater. Chem. Phys.*, 2009, **113**(2–3), 919–926, DOI: 10.1016/j.matchemphys.2008.08.065.

46 J. M. Thomassin, C. Pagnoulle, L. Bednarz, I. Huynen, R. Jerome and C. Detrembleur, Foams of polycaprolactone/MWNT nanocomposites for efficient EMI reduction, *J. Mater. Chem.*, 2008, **18**(7), 792–796, DOI: 10.1039/b709864b.

47 X. Yang, *et al.*, Synchronously improved electromagnetic interference shielding and thermal conductivity for epoxy nanocomposites by constructing 3D copper nanowires/thermally annealed graphene aerogel framework, *Composites, Part A*, 2020, **128**, 105670, DOI: 10.1016/j.compositesa.2019.105670.

48 X. Zhao, W. Xu, W. Yi and Y. Peng, A flexible and highly pressure-sensitive PDMS sponge based on silver nanoparticles decorated reduced graphene oxide composite, *Sens. Actuators, A*, 2019, **291**, 23–31, DOI: 10.1016/j.sna.2019.03.038.

49 M. Bayat, H. Yang, F. K. Ko, D. Michelson and A. Mei, Electromagnetic interference shielding effectiveness of hybrid multifunctional Fe$_3$O$_4$/carbon nanofiber composite, *Polymer*, 2014, **55**(3), 936–943, DOI: 10.1016/j.polymer.2013.12.042.

50 Y. Zhan, *et al.*, Fabrication of a flexible electromagnetic interference shielding Fe$_3$O$_4$@reduced graphene oxide/natural rubber composite with segregated network, *Chem. Eng. J.*, 2018, **344**, 184–193, DOI: 10.1016/j.cej.2018.03.085.

51 Y. Bhattacharjee and S. Bose, Core–Shell Nanomaterials for Microwave Absorption and Electromagnetic Interference Shielding: A Review, *ACS Appl. Nano Mater.*, 2021, **4**(2), 949–972, DOI: 10.1021/acsanm.1c00278.

52 S. Zeng, *et al.*, Flexible PVDF/CNTs/Ni@CNTs composite films possessing excellent electromagnetic interference shielding and mechanical properties under heat treatment, *Carbon*, 2019, **155**, 34–43, DOI: 10.1016/j.carbon.2019.08.024.

53 P. Xu, X. Han, J. Jiang, X. Wang, X. Li and A. Wen, Synthesis and characterization of novel coralloid polyaniline/BaFe 12O19 nanocomposites, *J. Phys. Chem. C*, 2007, **111**(34), 12603–12608, DOI: 10.1021/jp073872x.

54 W. Wang, S. P. Gumfekar, Q. Jiao and B. Zhao, Ferrite-grafted polyaniline nanofibers as electromagnetic shielding materials, *J. Mater. Chem. C*, 2013, **1**(16), 2851–2859, DOI: 10.1039/c3tc00757j.

55 S. Zhang, Y. Wang, Q. Ran, Q. Fu and Y. Gu, Electromagnetic interference shielding property of polybenzoxazine/graphene/nickel composites, *React.*

Funct. Polym., 2019, **143**, 104324, DOI: **10.1016/j.reactfunctpolym.2019.104324**.

56 I. Arief, S. Biswas and S. Bose, FeCo-Anchored Reduced Graphene Oxide Framework-Based Soft Composites Containing Carbon Nanotubes as Highly Efficient Microwave Absorbers with Excellent Heat Dissipation Ability, *ACS Appl. Mater. Interfaces*, 2017, **9**(22), 19202–19214, DOI: **10.1021/acsami.7b04053**.

57 S. Gao, S. H. Yang, H. Y. Wang, G. S. Wang and P. G. Yin, Excellent electromagnetic wave absorbing properties of two-dimensional carbon-based nanocomposite supported by transition metal carbides Fe_3C, *Carbon*, 2020, **162**, 438–444, DOI: **10.1016/j.carbon.2020.02.031**.

58 A. A. Al-Ghamdi, *et al.*, Conductive carbon black/magnetite hybrid fillers in microwave absorbing composites based on natural rubber, *Composites, Part B*, 2016, **96**, 231–241, DOI: **10.1016/j.compositesb.2016.04.039**.

59 S. Biswas, I. Arief, S. S. Panja and S. Bose, Electromagnetic screening in soft conducting composite-containing ferrites: The key role of size and shape anisotropy, *Mater. Chem. Front.*, 2017, **1**(12), 2574–2589, DOI: **10.1039/c7qm00305f**.

60 S. Biswas, S. S. Panja and S. Bose, Physical Insight into the Mechanism of Electromagnetic Shielding in Polymer Nanocomposites Containing Multiwalled Carbon Nanotubes and Inverse-Spinel Ferrites, *J. Phys. Chem. C*, 2018, **122**(34), 19425–19437, DOI: **10.1021/acs.jpcc.8b05867**.

61 G. Sang, *et al.*, Electromagnetic interference shielding performance of polyurethane composites: A comparative study of $GNs-IL/Fe_3O_4$ and $MWCNTs-IL/Fe_3O_4$ hybrid fillers, *Composites, Part B*, 2019, **164**, 467–475, DOI: **10.1016/j.compositesb.2019.01.062**.

62 H. Cheng, *et al.*, Synergetic effect of Fe_3O_4 nanoparticles and carbon on flexible poly(vinylidence fluoride) based films with higher heat dissipation to improve electromagnetic shielding, *Composites, Part A*, 2019, **121**, 139–148, DOI: **10.1016/j.compositesa.2019.03.019**.

63 S. P. Pawar, M. Gandi and S. Bose, High performance electromagnetic wave absorbers derived from PC/SAN blends containing multiwall carbon nanotubes and Fe_3O_4 decorated onto graphene oxide sheets, *RSC Adv.*, 2016, **6**(44), 37633–37645, DOI: **10.1039/c5ra25435c**.

64 J. Wu, Z. Ye, H. Ge, J. Chen, W. Liu and Z. Liu, Modified carbon fiber/magnetic graphene/epoxy composites with synergistic effect for electromagnetic interference shielding over broad frequency band, *J. Colloid Interface Sci.*, 2017, **506**, 217–226, DOI: **10.1016/j.jcis.2017.07.020**.

65 K. Sushmita, A. V. Menon, S. Sharma, A. C. Abhyankar, G. Madras and S. Bose, Mechanistic Insight into the Nature of Dopants in Graphene Derivatives Influencing Electromagnetic Interference Shielding Properties in Hybrid Polymer Nanocomposites, *J. Phys. Chem. C*, 2019, **123**(4), 2579–2590, DOI: **10.1021/acs.jpcc.8b10999**.

66 W. C. Yu, *et al.*, Superior and highly absorbed electromagnetic interference shielding performance achieved by designing the reflection-absorption-integrated shielding compartment with conductive wall and lossy core, *Chem. Eng. J.*, 2020, **393**, 124644, DOI: **10.1016/j.cej.2020.124644**.

67 R. S. Yadav, *et al.*, Lightweight $NiFe_2O_4$-Reduced Graphene Oxide-Elastomer Nanocomposite flexible sheet for electromagnetic interference shielding application, *Composites, Part B*, 2019, **166**, 95–111, DOI: **10.1016/j.compositesb.2018.11.069**.

68 G. Datt, C. Kotabage and A. C. Abhyankar, Ferromagnetic resonance of $NiCoFe_2O_4$ nanoparticles and microwave absorption properties of flexible $NiCoFe_2O_4$-carbon black/poly(vinyl alcohol) composites, *Phys. Chem. Chem. Phys.*, 2017, **19**(31), 20699–20712, DOI: **10.1039/c7cp03953k**.

69 A. Kobyliukh, K. Olszowska, U. Szeluga and S. Pusz, Iron oxides/graphene hybrid structures – Preparation, modification, and application as fillers of polymer composites, *Adv. Colloid Interface Sci.*, 2020, **285**, 102285, DOI: **10.1016/j.cis.2020.102285**.

70 X. Li, Z. Sun, Y. Zhang, D. Huang and J. Hu, Effects of oxygen vacancies on dielectric properties and relaxor behavior of Ba(ZrxTi1-x)O3 ceramics, *J. Phys.: Conf. Ser.*, 2021, **2101**(1), 012050, DOI: **10.1088/1742-6596/2101/1/012050**.

71 E. Cockayne, Influence of oxygen vacancies on the dielectric properties of hafnia: First-principles calculations, *Phys. Rev. B: Condens. Matter Mater. Phys.*, 2007, **75**(9), 1–8, DOI: **10.1103/PhysRevB.75.094103**.

72 B. K. Sahu and A. Das, Significance of in-plane oxygen vacancy rich non-stoichiometric layer towards unusual high dielectric constant in nano-structured SnO2, *Phys. E*, 2018, **103**, 60–65, DOI: **10.1016/j.physe.2018.05.016**.

73 M. D. Li, *et al.*, Oxygen-vacancy-related dielectric relaxation behaviours and impedance spectroscopy of Bi(Mg1/2Ti1/2)O3 modified BaTiO3 ferroelectric ceramics, *J. Mater.*, 2018, **4**(3), 194–201, DOI: **10.1016/j.jmat.2018.03.001**.

74 S. Biswas, Y. Bhattacharjee, S. S. Panja and S. Bose, Graphene oxide co-doped with dielectric and magnetic phases as an electromagnetic wave suppressor, *Mater. Chem. Front.*, 2017, **1**(6), 1229–1244, DOI: **10.1039/c6qm00335d**.

75 L. Jin, X. Zhao, J. Xu, Y. Luo, D. Chen and G. Chen, The synergistic effect of a graphene nanoplate/Fe_3O_4@$BaTiO_3$ hybrid and MWCNTs on enhancing broadband electromagnetic interference shielding performance, *RSC Adv.*, 2018, **8**(4), 2065–2071, DOI: **10.1039/c7ra12909b**.

76 P. Sambyal, S. K. Dhawan, P. Gairola, S. S. Chauhan and S. P. Gairola, Synergistic effect of polypyrrole/BST/RGO/Fe_3O_4 composite for enhanced microwave absorption and EMI shielding in X-Band, *Curr. Appl. Phys.*, 2018, **18**(5), 611–618, DOI: **10.1016/j.cap.2018.03.001**.

77 S. Das, S. Sharma, T. Yokozeki and S. Dhakate, "Conductive layer-based multifunctional structural composites for electromagnetic interference shielding, *Compos. Struct.*, 2021, **261**, 113293, DOI: **10.1016/j.compstruct.2020.113293**.

78 X. Jin, *et al.*, Flame-retardant poly(vinyl alcohol)/MXene multilayered films with outstanding electromagnetic interference shielding and thermal conductive
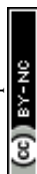
performances", *Chem. Eng. J.*, 2020, **380**, 122475, DOI: **10.1016/j.cej.2019.122475**.

79 Y. Bhattacharjee, I. Arief and S. Bose, Recent trends in multi-layered architectures towards screening electromagnetic radiation: Challenges and perspectives, *J. Mater. Chem. C*, 2017, **5**(30), 7390–7403, DOI: **10.1039/c7tc02172k**.

80 J. H. Lin, Z. I. Lin, Y. J. Pan, C. L. Huang, C. K. Chen and C. W. Lou, Polymer composites made of multi-walled carbon nanotubes and graphene nano-sheets: Effects of sandwich structures on their electromagnetic interference shielding effectiveness, *Composites, Part B*, 2016, **89**, 424–431, DOI: **10.1016/j.compositesb.2015.11.014**.

81 L. Q. Zhang, *et al.*, Tunable electromagnetic interference shielding effectiveness *via* multilayer assembly of regenerated cellulose as a supporting substrate and carbon nanotubes/polymer as a functional layer, *J. Mater. Chem. C*, 2017, **5**(12), 3130–3138, DOI: **10.1039/c6tc05516h**.

82 Y. Hu, P. Tang, L. Li, J. Yang, X. Jian and Y. Bin, High absorption shielding material of poly(phthalazinone etherketone)/multiwall carbon nanotube composite films with sandwich configurations, *RSC Adv.*, 2019, **9**(33), 18758–18766, DOI: **10.1039/c9ra02959a**.

83 S. Pande, B. P. Singh, R. B. Mathur, T. L. Dhami, P. Saini and S. K. Dhawan, Improved electromagnetic interference shielding properties of MWCNT-PMMA composites using layered structures, *Nanoscale Res. Lett.*, 2009, **4**(4), 327–334, DOI: **10.1007/s11671-008-9246-x**.

84 X. Feng, *et al.*, High Electromagnetic Interference Shielding Effectiveness of Carbon Nanotube–Cellulose Composite Films with Layered Structures, *Macromol. Mater. Eng.*, 2018, **303**(11), 1–8, DOI: **10.1002/mame.201800377**.

85 Q. Qi, *et al.*, An Effective Design Strategy for the Sandwich Structure of PVDF/GNP-Ni-CNT Composites with Remarkable Electromagnetic Interference Shielding Effectiveness, *ACS Appl. Mater. Interfaces*, 2020, **12**(32), 36568–36577, DOI: **10.1021/acsami.0c10600**.

86 Y. Xu, Y. Yang, D. X. Yan, H. Duan, G. Zhao and Y. Liu, Flexible and conductive polyurethane composites for electromagnetic shielding and printable circuit, *Chem. Eng. J.*, 2019, **360**, 1427–1436, DOI: **10.1016/j.cej.2018.10.235**.

87 X. Zhang, *et al.*, Ordered multilayer film of (graphene oxide/polymer and boron nitride/polymer) nanocomposites: An ideal EMI shielding material with excellent electrical insulation and high thermal conductivity, *Compos. Sci. Technol.*, 2016, **136**, 104–110, DOI: **10.1016/j.compscitech.2016.10.008**.

88 Y. Zhan, *et al.*, An anisotropic layer-by-layer carbon nanotube/boron nitride/rubber composite and its application in electromagnetic shielding, *Nanoscale*, 2020, **12**(14), 7782–7791, DOI: **10.1039/c9nr10672c**.

89 Y. Bhattacharjee, V. Bhingardive, S. Biswas and S. Bose, Construction of a carbon fiber based layer-by-layer (LbL) assembly-a smart approach towards effective EMI shielding, *RSC Adv.*, 2016, **6**(113), 112614–112619, DOI: **10.1039/C6RA24238C**.

90 S. Biswas, S. S. Panja and S. Bose, Unique Multilayered Assembly Consisting of 'flower-Like' Ferrite Nanoclusters Conjugated with MWCNT as Millimeter Wave Absorbers, *J. Phys. Chem. C*, 2017, **121**(26), 13998–14009, DOI: **10.1021/acs.jpcc.7b02668**.

91 I. Arief, Y. Bhattacharjee, O. Prakash, M. Sahu, S. Suwas and S. Bose, Tunable CoNi microstructures in flexible multilayered polymer films can shield electromagnetic radiation, *Composites, Part B*, 2019, **177**, 107283, DOI: **10.1016/j.compositesb.2019.107283**.

92 S. Li, Z. Xu, Y. Dong, D. Liu and G. Sui, Ni@nylon mesh/PP composites with a novel tree-ring structure for enhancing electromagnetic shielding, *Composites, Part A*, 2020, **131**, 105798, DOI: **10.1016/j.compositesa.2020.105798**.

93 J. D. Sudha, S. Sivakala, K. Patel and P. Radhakrishnan Nair, Development of electromagnetic shielding materials from the conductive blends of polystyrene polyaniline-clay nanocomposite, *Composites, Part A*, 2010, **41**(11), 1647–1652, DOI: **10.1016/j.compositesa.2010.07.015**.

94 Y. Xu, Y. Yang, D. X. Yan, H. Duan, G. Zhao and Y. Liu, Gradient Structure Design of Flexible Waterborne Polyurethane Conductive Films for Ultraefficient Electromagnetic Shielding with Low Reflection Characteristic, *ACS Appl. Mater. Interfaces*, 2018, **10**(22), 19143–19152, DOI: **10.1021/acsami.8b05129**.

95 H. Duan, *et al.*, Effect of carbon nanofiller dimension on synergistic EMI shielding network of epoxy/metal conductive foams, *Composites, Part A*, 2019, **118**, 41–48, DOI: **10.1016/j.compositesa.2018.12.016**.

96 W. Ren, *et al.*, Flexible and robust silver coated non-woven fabric reinforced waterborne polyurethane films for ultra-efficient electromagnetic shielding, *Composites, Part B*, 2020, **184**, 107745, DOI: **10.1016/j.compositesb.2020.107745**.

97 J. Yang, *et al.*, Gradient structure design of lightweight and flexible silicone rubber nanocomposite foam for efficient electromagnetic interference shielding, *Chem. Eng. J.*, 2020, **390**, 124589, DOI: **10.1016/j.cej.2020.124589**.

98 H. Duan, *et al.*, Asymmetric conductive polymer composite foam for absorption dominated ultra-efficient electromagnetic interference shielding with extremely low reflection characteristics, *J. Mater. Chem. A*, 2020, **8**(18), 9146–9159, DOI: **10.1039/d0ta01393e**.

99 A. Sheng, *et al.*, Multilayer WPU conductive composites with controllable electro-magnetic gradient for absorption-dominated electromagnetic interference shielding, *Composites, Part A*, 2020, **129**, 105692, DOI: **10.1016/j.compositesa.2019.105692**.

100 H. J. Im, J. Y. Oh, S. Ryu and S. H. Hong, The design and fabrication of a multilayered graded GNP/Ni/PMMA nanocomposite for enhanced EMI shielding behavior, *RSC Adv.*, 2019, **9**(20), 11289–11295, DOI: **10.1039/C9RA00573K**.

101 M. Y. Yablokov, V. G. Shevchenko, L. A. Mukhortov and A. N. Ozerin, Electromagnetic interference shielding of carbon nanotube-fluoropolymer elastomer composites with layered structure, *Fullerenes, Nanotubes Carbon*
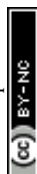
Nanostruct., 2020, **28**(4), 267–271, DOI: **10.1080/1536383X.2019.1697685**.

102 Y. Cai, *et al.*, Electrical conductivity and electromagnetic shielding properties of Ti3SiC2/SiC functionally graded materials prepared by positioning impregnation, *J. Eur. Ceram. Soc.*, 2019, **39**(13), 3643–3650, DOI: **10.1016/j.jeurceramsoc.2019.05.039**.

103 M. Chen, Y. Zhu, Y. Pan, H. Kou, H. Xu and J. Guo, Gradient multilayer structural design of CNTs/SiO2 composites for improving microwave absorbing properties, *Mater. Des.*, 2011, **32**(5), 3013–3016, DOI: **10.1016/j.matdes.2010.12.043**.

104 X. Ma, Q. Zhang, Z. Luo, X. Lin and G. Wu, A novel structure of Ferro-Aluminum based sandwich composite for magnetic and electromagnetic interference shielding, *Mater. Des.*, 2016, **89**, 71–77, DOI: **10.1016/j.matdes.2015.09.137**.

105 R. Kumar, *et al.*, Heteroatom doping of 2D graphene materials for electromagnetic interference shielding: a review of recent progress, *Crit. Rev. Solid State Mater. Sci.*, 2021, **0**(0), 1–50, DOI: **10.1080/10408436.2021.1965954**.

106 N. Chen, X. Huang and L. Qu, Heteroatom substituted and decorated graphene: Preparation and applications, *Phys. Chem. Chem. Phys.*, 2015, **17**(48), 32077–32098, DOI: **10.1039/c5cp04391c**.

107 Y. G. Zhou, X. T. Zu, F. Gao, H. Y. Xiao and H. F. Lv, Electronic and magnetic properties of graphene absorbed with S atom: A first principles study, *J. Appl. Phys.*, 2009, **105**(2), 104311, DOI: **10.1063/1.3130401**.

108 P. A. Denis, R. Faccio and A. W. Mombru, Is it possible to dope single walled carbon nanotubes and graphene with sulfur?, *ChemPhysChem*, 2009, **10**(4), 715–722, DOI: **10.1002/cphc.200800592**.

109 K. Zhang, J. Luo, N. Yu, M. Gu and X. Sun, Synthesis and excellent electromagnetic absorption properties of reduced graphene oxide/PANI/BaNd$_{0.2}$Sm$_{0.2}$Fe$_{11.6}$O$_{19}$ nanocomposites, *J. Alloys Compd.*, 2019, **779**, 270–279, DOI: **10.1016/j.jallcom.2018.11.284**.

110 Y. Zhang, *et al.*, Fabrication and investigation on the ultra-thin and flexible Ti$_3$C$_2$T$_x$/co-doped polyaniline electromagnetic interference shielding composite films, *Compos. Sci. Technol.*, 2019, **183**, 107833, DOI: **10.1016/j.compscitech.2019.107833**.

111 K. Zhang, J. Luo, N. Yu, M. Gu and X. Sun, Synthesis and excellent electromagnetic absorption properties of reduced graphene BaNd$_{0.2}$Sm$_{0.2}$Fe$_{11.6}$O$_{19}$ nanocomposites, *J. Alloys Compd.*, 2019, **779**, 270–279, DOI: **10.1016/j.jallcom.2018.11.284**.

112 S. Khasim, Polyaniline-Graphene nanoplatelet composite films with improved conductivity for high performance X-band microwave shielding applications, *Results Phys.*, 2019, **12**, 1073–1081, DOI: **10.1016/j.rinp.2018.12.087**.

113 T. Omura, C. H. Chan, M. Wakisaka and H. Nishida, Organic Thin Paper of Cellulose Nanofiber/Polyaniline Doped with (±)-10-Camphorsulfonic Acid Nanohybrid and Its Application to Electromagnetic Shielding, *ACS Omega*, 2019, **4**(5), 9446–9452, DOI: **10.1021/acsomega.9b00708**.

114 S. S. Seyyed Afghahi, R. Peymanfar, S. Javanshir, Y. Atassi and M. Jafarian, Synthesis, characterization and microwave characteristics of ternary nanocomposite of MWCNTs/doped Sr-hexaferrite/PANI, *J. Magn. Magn. Mater.*, 2017, **423**, 152–157, DOI: **10.1016/j.jmmm.2016.09.082**.

115 P. Chamoli, S. K. Singh, M. J. Akhtar, M. K. Das and K. K. Kar, Nitrogen doped graphene nanosheet-epoxy nanocomposite for excellent microwave absorption, *Phys. E*, 2018, **103**, 25–34, DOI: **10.1016/j.physe.2018.05.020**.

116 H. Kadkhodayan, M. S. Seyed Dorraji, M. H. Rasoulifard, A. R. Amani-Ghadim, I. Hajimiri and A. R. Tarighati Sareshkeh, Enhanced microwave absorption property of MnFe9n+3O15n+4(0 ≤ n ≤ 1) (M = Ba, Sr)/CaCu3Ti4O12/phosphorus-doped g-C3N4 nanocomposite: Preparation and optimization, *J. Alloys Compd.*, 2018, **735**(2018), 2497–2506, DOI: **10.1016/j.jallcom.2017.12.017**.

117 M. Saini, R. Shukla and A. Kumar, Cd2+ substituted nickel ferrite doped polyaniline nanocomposites as effective shield against electromagnetic radiation in X-band frequency, *J. Magn. Magn. Mater.*, 2019, **491**, 165549, DOI: **10.1016/j.jmmm.2019.165549**.

118 Y. F. Liu, L. M. Feng, Y. F. Chen, Y. D. Shi, X. D. Chen and M. Wang, Segregated polypropylene/cross-linked poly(ethylene-co-1-octene)/multi-walled carbon nanotube nanocomposites with low percolation threshold and dominated negative temperature coefficient effect: Towards electromagnetic interference shielding and thermisto, *Compos. Sci. Technol.*, 2018, **159**, 152–161, DOI: **10.1016/j.compscitech.2018.02.041**.

119 A. Nasr Esfahani, A. A. Katbab, A. Taeb, L. Simon and M. A. Pope, Correlation between mechanical dissipation and improved X-band electromagnetic shielding capabilities of amine functionalized graphene/thermoplastic polyurethane composites, *Eur. Polym. J.*, 2017, **95**, 520–538, DOI: **10.1016/j.eurpolymj.2017.08.038**.

120 J. Abraham, *et al.*, Investigation into dielectric behaviour and electromagnetic interference shielding effectiveness of conducting styrene butadiene rubber composites containing ionic liquid modified MWCNT, *Polymer*, 2017, **112**, 102–115, DOI: **10.1016/j.polymer.2017.01.078**.

121 J. P. Soares da Silva, B. G. Soares, S. Livi and G. M. O. Barra, Phosphonium–based ionic liquid as dispersing agent for MWCNT in melt-mixing polystyrene blends: Rheology, electrical properties and EMI shielding effectiveness, *Mater. Chem. Phys.*, 2017, **189**, 162–168, DOI: **10.1016/j.matchemphys.2016.12.073**.

122 T. Kaur, S. Kumar, S. B. Narang and A. K. Srivastava, Radiation losses in microwave Ku region by conducting pyrrole/barium titanate and barium hexaferrite based nanocomposites, *J. Magn. Magn. Mater.*, 2016, **420**, 336–342, DOI: **10.1016/j.jmmm.2016.07.058**.

123 S. Araby, A. Qiu, R. Wang, Z. Zhao, C. H. Wang and J. Ma, Aerogels based on carbon nanomaterials, *J. Mater. Sci.*, 2016, **51**(20), 9157–9189, DOI: **10.1007/s10853-016-0141-z**.

124 S. S. Kistler, Coherent expanded aerogels, *J. Phys. Chem.*, 1932, **36**(1), 52–64, DOI: **10.1021/j150331a003**.

125 P. Song, *et al.*, Lightweight, Flexible Cellulose-Derived Carbon Aerogel@Reduced Graphene Oxide/PDMS Composites with Outstanding EMI Shielding Performances and Excellent Thermal Conductivities, *Nano-Micro Lett.*, 2021, **13**(1), 1–17, DOI: **10.1007/s40820-021-00624-4**.

126 M. T. Noman, *et al.*, Aerogels for biomedical, energy and sensing applications, *Gels*, 2021, **7**(4), 1–17, DOI: **10.3390/gels7040264**.

127 L. Wang, H. Xu, J. Gao, J. Yao and Q. Zhang, Recent progress in metal-organic frameworks-based hydrogels and aerogels and their applications, *Coord. Chem. Rev.*, 2019, **398**, 213016, DOI: **10.1016/j.ccr.2019.213016**.

128 F. Xie, K. Gao, L. Zhuo, F. Jia, Q. Ma and Z. Lu, Robust $Ti_3C_2T_x$/RGO/ANFs hybrid aerogel with outstanding electromagnetic shielding performance and compression resilience, *Composites, Part A*, 2022, **160**, 107049, DOI: **10.1016/j.compositesa.2022.107049**.

129 P. Hu, *et al.*, Multifunctional Aramid Nanofiber/Carbon Nanotube Hybrid Aerogel Films, *ACS Nano*, 2020, **14**(1), 688–697, DOI: **10.1021/acsnano.9b07459**.

130 S. Zhao, Y. Yan, A. Gao, S. Zhao, J. Cui and G. Zhang, Flexible Polydimethylsilane Nanocomposites Enhanced with a Three-Dimensional Graphene/Carbon Nanotube Bicontinuous Framework for High-Performance Electromagnetic Interference Shielding, *ACS Appl. Mater. Interfaces*, 2018, **10**(31), 26723–26732, DOI: **10.1021/acsami.8b09275**.

131 L. Q. Zhang, S. G. Yang, L. Li, B. Yang, H. D. Huang, D. X. Yan and Z. M. Li, Ultralight cellulose porous composites with manipulated porous structure and carbon nanotube distribution for promising electromagnetic interference shielding, *ACS Appl. Mater. Interfaces*, 2018, **10**(46), 40156–40167.

132 S. Zhao, *et al.*, Highly Electrically Conductive Three-Dimensional $Ti_3C_2T_x$ MXene/Reduced Graphene Oxide Hybrid Aerogels with Excellent Electromagnetic Interference Shielding Performances, *ACS Nano*, 2018, **12**(11), 11193–11202, DOI: **10.1021/acsnano.8b05739**.

133 F. Xu, *et al.*, Superflexible Interconnected Graphene Network Nanocomposites for High-Performance Electromagnetic Interference Shielding, *ACS Omega*, 2018, **3**(3), 3599–3607, DOI: **10.1021/acsomega.8b00432**.

134 Z. Zeng, *et al.*, Ultralight and Flexible Polyurethane/Silver Nanowire Nanocomposites with Unidirectional Pores for Highly Effective Electromagnetic Shielding, *ACS Appl. Mater. Interfaces*, 2017, **9**(37), 32211–32219, DOI: **10.1021/acsami.7b07643**.

135 X. H. Li, *et al.*, Thermally Annealed Anisotropic Graphene Aerogels and Their Electrically Conductive Epoxy Composites with Excellent Electromagnetic Interference Shielding Efficiencies, *ACS Appl. Mater. Interfaces*, 2016, **8**(48), 33230–33239, DOI: **10.1021/acsami.6b12295**.

136 X. Wu, *et al.*, Compressible, durable and conductive polydimethylsiloxane-coated MXene foams for high-performance electromagnetic interference shielding, *Chem. Eng. J.*, 2020, **381**, 122622, DOI: **10.1016/j.cej.2019.122622**.

137 W. Gao, *et al.*, High-efficiency electromagnetic interference shielding realized in nacre-mimetic graphene/polymer composite with extremely low graphene loading, *Carbon*, 2020, **157**, 570–577, DOI: **10.1016/j.carbon.2019.10.051**.

138 L. Wang, *et al.*, 3D $Ti_3C_2T_x$ MXene/C hybrid foam/epoxy nanocomposites with superior electromagnetic interference shielding performances and robust mechanical properties, *Composites, Part A*, 2019, **123**, 293–300, DOI: **10.1016/j.compositesa.2019.05.030**.

139 Y. Chen, H. Bin Zhang, M. Wang, X. Qian, A. Dasari and Z. Z. Yu, Phenolic resin-enhanced three-dimensional graphene aerogels and their epoxy nanocomposites with high mechanical and electromagnetic interference shielding performances, *Compos. Sci. Technol.*, 2017, **152**, 254–262, DOI: **10.1016/j.compscitech.2017.09.022**.

140 L. Ma, M. Hamidinejad, L. Wei, B. Zhao and C. B. Park, Absorption-dominant EMI shielding polymer composite foams: Microstructure and geometry optimization, *Mater. Today Phys.*, 2023, **30**, 100940, DOI: **10.1016/j.mtphys.2022.100940**.

141 J. F. Wang, S. Q. Shi, J. P. Yang and W. Zhang, Multiscale analysis on free vibration of functionally graded graphene reinforced PMMA composite plates, *Appl. Math. Model.*, 2021, **98**, 38–58, DOI: **10.1016/j.apm.2021.04.023**.

142 Y. Yang, M. C. Gupta, K. L. Dudley and R. W. Lawrence, Novel carbon nanotube – Polystyrene foam composites for electromagnetic interference shielding, *Nano Lett.*, 2005, **5**(11), 2131–2134, DOI: **10.1021/nl051375r**.

143 X. Ma, B. Shen, L. Zhang, Y. Liu, W. Zhai and W. Zheng, Porous superhydrophobic polymer/carbon composites for lightweight and self-cleaning EMI shielding application, *Compos. Sci. Technol.*, 2018, **158**, 86–93, DOI: **10.1016/j.compscitech.2018.02.006**.

144 H. Zhang, G. Zhang, Q. Gao, M. Zong, M. Wang and J. Qin, Electrically electromagnetic interference shielding microcellular composite foams with 3D hierarchical graphene-carbon nanotube hybrids, *Composites, Part A*, 2020, **130**, 105773, DOI: **10.1016/j.compositesa.2020.105773**.

145 H. Zhang, *et al.*, Multifunctional microcellular PVDF/Ni-chains composite foams with enhanced electromagnetic interference shielding and superior thermal insulation performance, *Chem. Eng. J.*, 2020, **379**, 122304, DOI: **10.1016/j.cej.2019.122304**.

146 J. Yang, *et al.*, Light-weight and flexible silicone rubber/MWCNTs/Fe_3O_4 nanocomposite foams for efficient electromagnetic interference shielding and microwave absorption, *Compos. Sci. Technol.*, 2019, **181**, 107670, DOI: **10.1016/j.compscitech.2019.05.027**.

147 L. Liu, H. Wang, M. Shan, Y. Jiang, X. Zhang and Z. Xu, Lightweight sandwich fiber-welded foam-like nonwoven fabrics/graphene composites for electromagnetic shielding, *Mater. Chem. Phys.*, 2019, **232**, 246–253, DOI: **10.1016/j.matchemphys.2019.04.085**.
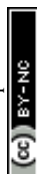
148 X. Fan, *et al.*, Study on foamability and electromagnetic interference shielding effectiveness of supercritical CO 2 foaming epoxy/rubber/MWCNTs composite, *Composites, Part A*, 2019, **121**, 64–73, DOI: **10.1016/j.compositesa.2019.03.008**.

149 H. Zhang, *et al.*, Synergistic effect of carbon nanotube and graphene nanoplates on the mechanical, electrical and electromagnetic interference shielding properties of polymer composites and polymer composite foams, *Chem. Eng. J.*, 2018, **353**, 381–393, DOI: **10.1016/j.cej.2018.07.144**.

150 H. Yuan, Y. Xiong, Q. Shen, G. Luo, D. Zhou and L. Liu, Synthesis and electromagnetic absorbing performances of CNTs/PMMA laminated nanocomposite foams in X-band, *Composites, Part A*, 2018, **107**, 334–341, DOI: **10.1016/j.compositesa.2018.01.024**.

151 S. E. Zakiyan, H. Azizi and I. Ghasemi, Effect of cell morphology on electrical properties and electromagnetic interference shielding of graphene-poly(methyl methacrylate) microcellular foams, *Compos. Sci. Technol.*, 2018, **157**, 217–227, DOI: **10.1016/j.compscitech.2018.02.002**.

152 J. Li, *et al.*, Electrical conductivity and electromagnetic interference shielding of epoxy nanocomposite foams containing functionalized multi-wall carbon nanotubes, *Appl. Surf. Sci.*, 2018, **428**, 7–16, DOI: **10.1016/j.apsusc.2017.08.234**.

153 H. Zhang, *et al.*, Lightweight, multifunctional microcellular PMMA/Fe$_3$O$_4$@MWCNTs nanocomposite foams with efficient electromagnetic interference shielding, *Composites, Part A*, 2017, **100**, 128–138, DOI: **10.1016/j.compositesa.2017.05.009**.

154 M. Soltani Alkuh, M. H. N. Famili, M. Mokhtari Motameni Shirvan and M. H. Moeini, The relationship between electromagnetic absorption properties and cell structure of poly(methyl methacrylate)/multi-walled carbon nanotube composite foams, *Mater. Des.*, 2016, **100**, 73–83, DOI: **10.1016/j.matdes.2016.03.075**.

155 J. Li, *et al.*, Morphologies and electromagnetic interference shielding performances of microcellular epoxy/multi-wall carbon nanotube nanocomposite foams, *Compos. Sci. Technol.*, 2016, **129**, 70–78, DOI: **10.1016/j.compscitech.2016.04.003**.

156 G. Gedler, M. Antunes, J. I. Velasco and R. Ozisik, Enhanced electromagnetic interference shielding effectiveness of polycarbonate/graphene nanocomposites foamed *via* 1-step supercritical carbon dioxide process, *Mater. Des.*, 2016, **90**, 906–914, DOI: **10.1016/j.matdes.2015.11.021**.

157 B. Zhao, *et al.*, Achieving wideband microwave absorption properties in PVDF nanocomposite foams with an ultra-low MWCNT content by introducing a microcellular structure, *J. Mater. Chem. C*, 2019, **8**(1), 58–70, DOI: **10.1039/c9tc04575a**.

158 B. Zhao, *et al.*, Incorporating a microcellular structure into PVDF/graphene-nanoplatelet composites to tune their electrical conductivity and electromagnetic interference shielding properties, *J. Mater. Chem. C*, 2018, **6**(38), 10292–10300, DOI: **10.1039/C8TC03714K**.

159 F. Huang, *et al.*, Oxidized multiwall carbon nanotube/silicone foam composites with effective electromagnetic interference shielding and high gamma radiation stability, *RSC Adv.*, 2018, **8**(43), 24236–24242, DOI: **10.1039/c8ra03314e**.

160 C. Zhang, *et al.*, Facile fabrication of ultra-light and highly resilient PU/RGO foams for microwave absorption, *RSC Adv.*, 2017, **7**(66), 41321–41329, DOI: **10.1039/c7ra07794g**.

161 C. Liang, *et al.*, Constructing interconnected spherical hollow conductive networks in silver platelets/reduced graphene oxide foam/epoxy nanocomposites for superior electromagnetic interference shielding effectiveness, *Nanoscale*, 2019, **11**(46), 22590–22598, DOI: **10.1039/c9nr06022g**.

162 X. Sun, X. Liu, X. Shen, Y. Wu, Z. Wang and J. K. Kim, Graphene foam/carbon nanotube/poly(dimethyl siloxane) composites for exceptional microwave shielding, *Composites, Part A*, 2016, **85**, 199–206, DOI: **10.1016/j.compositesa.2016.03.009**.

163 J. Liu, J. Cheng, R. Che, J. Xu, M. Liu and Z. Liu, Double-shelled yolk-shell microspheres with Fe$_3$O$_4$ cores and SnO2 double shells as high-performance microwave absorbers, *J. Phys. Chem. C*, 2013, **117**(1), 489–495, DOI: **10.1021/jp310898z**.

164 I. Arief, S. Biswas and S. Bose, Wool-Ball-Type Core-Dual-Shell FeCo@SiO2@MWCNTs Microcubes for Screening Electromagnetic Interference, *ACS Appl. Nano Mater.*, 2018, **1**(5), 2261–2271, DOI: **10.1021/acsanm.8b00333**.

165 L. yan Li, S. lin Li, Y. Shao, R. Dou, B. Yin and M. bo Yang, PVDF/PS/HDPE/MWCNTs/Fe$_3$O$_4$ nanocomposites: Effective and lightweight electromagnetic interference shielding material through the synergetic effect of MWCNTs and Fe$_3$O$_4$ nanoparticles, *Curr. Appl. Phys.*, 2018, **18**(4), 388–396, DOI: **10.1016/j.cap.2018.01.014**.

166 K. Manna and S. K. Srivastava, Fe$_3$O$_4$@Carbon@Polyaniline Trilaminar Core–Shell Composites as Superior Microwave Absorber in Shielding of Electromagnetic Pollution, *ACS Sustain. Chem. Eng.*, 2017, **5**(11), 10710–10721, DOI: **10.1021/acssuschemeng.7b02682**.

167 S. Li, Y. Huang, N. Zhang, M. Zong and P. Liu, Synthesis of polypyrrole decorated FeCo@SiO2 as a high-performance electromagnetic absorption material, *J. Alloys Compd.*, 2019, **774**, 532–539, DOI: **10.1016/j.jallcom.2018.09.349**.

168 Y. Bhattacharjee, D. Chatterjee and S. Bose, Core-Multishell Heterostructure with Excellent Heat Dissipation for Electromagnetic Interference Shielding, *ACS Appl. Mater. Interfaces*, 2018, **10**(36), 30762–30773, DOI: **10.1021/acsami.8b10819**.

169 L. Wang, *et al.*, Electromagnetic interference shielding MWCNT-Fe$_3$O$_4$@Ag/epoxy nanocomposites with satisfactory thermal conductivity and high thermal stability, *Carbon*, 2019, **141**, 506–514, DOI: **10.1016/j.carbon.2018.10.003**.

170 Y. Yuan, *et al.*, Lightweight, flexible and strong core–shell non-woven fabrics covered by reduced graphene oxide for
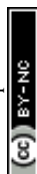
high-performance electromagnetic interference shielding, *Carbon*, 2018, **130**, 59–68, DOI: **10.1016/j.carbon.2017.12.122**.

171 Y. Wang, W. Zhang, C. Luo, X. Wu, G. Yan and W. Chen, Fabrication and high-performance microwave absorption of Ni@SnO2@PPy Core–Shell composite, *Synth. Met.*, 2016, **220**, 347–355, DOI: **10.1016/j.synthmet.2016.07.005**.

172 H. K. Choudhary, R. Kumar, S. P. Pawar, U. Sundararaj and B. Sahoo, Enhancing absorption dominated microwave shielding in co@c-pvdf nanocomposites through improved magnetization and graphitization of the co@c-nanoparticles, *Phys. Chem. Chem. Phys.*, 2019, **21**(28), 15595–15608, DOI: **10.1039/c9cp03305j**.

173 K. Zhang, *et al.*, A facile approach to constructing efficiently segregated conductive networks in poly(lactic acid)/silver nanocomposites *via* silver plating on microfibers for electromagnetic interference shielding, *Compos. Sci. Technol.*, 2018, **156**, 136–143, DOI: **10.1016/j.compscitech.2017.12.037**.

174 X. P. Zhang, L. C. Jia, G. Zhang, D. X. Yan and Z. M. Li, A highly efficient and heat-resistant electromagnetic interference shielding carbon nanotube/poly(phenylene sulfide) composite *via* sinter molding, *J. Mater. Chem. C*, 2018, **6**(40), 10760–10766, DOI: **10.1039/C8TC03493A**.

175 R. Sun, *et al.*, Highly Conductive Transition Metal Carbide/Carbonitride(MXene)@polystyrene Nanocomposites Fabricated by Electrostatic Assembly for Highly Efficient Electromagnetic Interference Shielding, *Adv. Funct. Mater.*, 2017, **27**(45), 1–11, DOI: **10.1002/adfm.201702807**.

176 J. Ju, *et al.*, Lightweight multifunctional polypropylene/carbon nanotubes/carbon black nanocomposite foams with segregated structure, ultralow percolation threshold and enhanced electromagnetic interference shielding performance, *Compos. Sci. Technol.*, 2020, **193**, 108116, DOI: **10.1016/j.compscitech.2020.108116**.

177 J. Chen, X. Liao, W. Xiao, J. Yang, Q. Jiang and G. Li, Facile and Green Method to Structure Ultralow-Threshold and Lightweight Polystyrene/MWCNT Composites with Segregated Conductive Networks for Efficient Electromagnetic Interference Shielding, *ACS Sustain. Chem. Eng.*, 2019, **7**(11), 9904–9915, DOI: **10.1021/acssuschemeng.9b00678**.

178 Y. J. Tan, *et al.*, Comparative study on solid and hollow glass microspheres for enhanced electromagnetic interference shielding in polydimethylsiloxane/multi-walled carbon nanotube composites, *Composites, Part B*, 2019, **177**(August), 107378, DOI: **10.1016/j.compositesb.2019.107378**.

179 F. Sharif, M. Arjmand, A. A. Moud, U. Sundararaj and E. P. L. Roberts, Segregated Hybrid Poly(methyl methacrylate)/Graphene/Magnetite Nanocomposites for Electromagnetic Interference Shielding, *ACS Appl. Mater. Interfaces*, 2017, **9**(16), 14171–14179, DOI: **10.1021/acsami.6b13986**.

180 Y. Zhan, *et al.*, Enhancing the EMI shielding of natural rubber-based supercritical CO 2 foams by exploiting their porous morphology and CNT segregated networks,

Nanoscale, 2019, **11**(3), 1011–1020, DOI: **10.1039/c8nr07351a**.

181 W. C. Yu *et al.*, Constructing highly oriented segregated structure towards high-strength carbon nanotube/ultrahigh-molecular-weight polyethylene composites for electromagnetic interference shielding, **110**, Elsevier Ltd, 2018.

182 K. Zhang, *et al.*, A facile approach to constructing efficiently segregated conductive networks in poly(lactic acid)/silver nanocomposites *via* silver plating on microfibers for electromagnetic interference shielding, *Compos. Sci. Technol.*, 2018, **156**, 136–143, DOI: **10.1016/j.compscitech.2017.12.037**.

183 H. Wang, *et al.*, 3D network porous polymeric composites with outstanding electromagnetic interference shielding, *Compos. Sci. Technol.*, 2016, **125**, 22–29, DOI: **10.1016/j.compscitech.2016.01.007**.

184 K. Zhang, *et al.*, Ultralow percolation threshold and enhanced electromagnetic interference shielding in poly(l-lactide)/multi-walled carbon nanotube nanocomposites with electrically conductive segregated networks, *J. Mater. Chem. C*, 2017, **5**(36), 9359–9369, DOI: **10.1039/c7tc02948a**.

185 P. Song, *et al.*, Honeycomb structural rGO-MXene/epoxy nanocomposites for superior electromagnetic interference shielding performance, *Sustainable Mater. Technol.*, 2020, **24**, e00153, DOI: **10.1016/j.susmat.2020.e00153**.

186 V. T. Nguyen, B. K. Min, Y. Yi, S. J. Kim and C. G. Choi, MXene(Ti$_3$C$_2$T$_x$)/graphene/PDMS composites for multifunctional broadband electromagnetic interference shielding skins, *Chem. Eng. J.*, 2020, **393**, 124608, DOI: **10.1016/j.cej.2020.124608**.

187 F. Shahzad, Electromagnetic interference shielding with 2D transition metal carbides (MXenes), *Science*, 2016, **353**(6304), 1137–1140, DOI: **10.1126/science.aag2421**.

188 P. Song, *et al.*, Obviously improved electromagnetic interference shielding performances for epoxy composites *via* constructing honeycomb structural reduced graphene oxide, *Compos. Sci. Technol.*, 2019, **181**, 107698, DOI: **10.1016/j.compscitech.2019.107698**.

189 H. Fang, H. Guo, Y. Hu, Y. Ren, P. C. Hsu and S. L. Bai, *In situ* grown hollow Fe$_3$O$_4$ onto graphene foam nanocomposites with high EMI shielding effectiveness and thermal conductivity, *Compos. Sci. Technol.*, 2020, **188**, 107975, DOI: **10.1016/j.compscitech.2019.107975**.

190 C. Liang, *et al.*, Highly oriented three-dimensional structures of Fe$_3$O$_4$ decorated CNTs/reduced graphene oxide foam/epoxy nanocomposites against electromagnetic pollution, *Compos. Sci. Technol.*, 2019, **181**, 107683, DOI: **10.1016/j.compscitech.2019.107683**.

191 Y. Huangfu, *et al.*, Fabrication and investigation on the PANI/MWCNT/thermally annealed graphene aerogel/epoxy electromagnetic interference shielding nanocomposites, *Composites, Part A*, 2019, **121**, 265–272, DOI: **10.1016/j.compositesa.2019.03.041**.

192 Y. Huangfu, *et al.*, Fabrication and investigation on the Fe$_3$O$_4$/thermally annealed graphene aerogel/epoxy

electromagnetic interference shielding nanocomposites, *Compos. Sci. Technol.*, 2019, **169**, 70–75, DOI: **10.1016/j.compscitech.2018.11.012**.

193 J. Ouyang, Q. Xu, C. W. Chu, Y. Yang, G. Li and J. Shinar, On the mechanism of conductivity enhancement in poly(3,4-ethylenedioxythiophene):poly(styrene sulfonate) film through solvent treatment, *Polymer*, 2004, **45**(25), 8443–8450, DOI: **10.1016/j.polymer.2004.10.001**.

194 D. Zheng, G. Tang, H. B. Zhang, Z. Z. Yu, F. Yavari, N. Koratkar, S. H. Lim and M. W. Lee, In situ thermal reduction of graphene oxide for high electrical conductivity and low percolation threshold in polyamide 6 nanocomposites, *Compos. Sci. Technol.*, 2012, **72**(2), 284–289, DOI: **10.1016/j.compscitech.2011.11.014**.

195 C. Lan, M. Guo, C. Li, Y. Qiu, Y. Ma and J. Sun, Axial Alignment of Carbon Nanotubes on Fibers to Enable Highly Conductive Fabrics for Electromagnetic Interference Shielding, *ACS Appl. Mater. Interfaces*, 2020, **12**(6), 7477–7485, DOI: **10.1021/acsami.9b21698**.

196 J. P L, H. Nallabothula, A. V. Menon and S. Bose, Nanoinfiltration for Enhancing Microwave Attenuation in Polystyrene-Nanoparticle Composites, *ACS Appl. Nano Mater.*, 2020, **3**(2), 1872–1880, DOI: **10.1021/acsanm.9b02521**.

197 R. Salehiyan, M. Nofar, S. S. Ray and V. Ojijo, Kinetically Controlled Localization of Carbon Nanotubes in Polylactide/Poly(vinylidene fluoride) Blend Nanocomposites and Their Influence on Electromagnetic Interference Shielding, Electrical Conductivity, and Rheological Properties, *J. Phys. Chem. C*, 2019, **123**(31), 19195–19207, DOI: **10.1021/acs.jpcc.9b04494**.

198 S. M. N. Sultana, S. P. Pawar and U. Sundararaj, Effect of Processing Techniques on EMI SE of Immiscible PS/PMMA Blends Containing MWCNT: Enhanced Intertube and Interphase Scattering, *Ind. Eng. Chem. Res.*, 2019, **58**(26), 11576–11584, DOI: **10.1021/acs.iecr.8b05957**.

199 H. Nallabothula, Y. Bhattacharjee, L. Samantara and S. Bose, Processing-Mediated Different States of Dispersion of Multiwalled Carbon Nanotubes in PDMS Nanocomposites Influence EMI Shielding Performance, *ACS Omega*, 2019, **4**(1), 1781–1790, DOI: **10.1021/acsomega.8b02920**.

200 S. P. Pawar, P. Rzeczkowski, P. Pötschke, B. Krause and S. Bose, Does the Processing Method Resulting in Different States of an Interconnected Network of Multiwalled Carbon Nanotubes in Polymeric Blend Nanocomposites Affect EMI Shielding Properties?, *ACS Omega*, 2018, **3**(5), 5771–5782, DOI: **10.1021/acsomega.8b00575**.

201 R. Rohini and S. Bose, Extraordinary Improvement in Mechanical Properties and Absorption-Driven Microwave Shielding through Epoxy-Grafted Graphene 'interconnects', *ACS Omega*, 2018, **3**(3), 3200–3210, DOI: **10.1021/acsomega.7b01997**.

202 W. Xu, Y. F. Pan, W. Wei and G. S. Wang, Nanocomposites of Oriented Nickel Chains with Tunable Magnetic Properties for High-Performance Broadband Microwave Absorption, *ACS Appl. Nano Mater.*, 2018, **1**(3), 1116–1123, DOI: **10.1021/acsanm.7b00293**.

203 J. Hua, *et al.*, Graphene/MWNT/Poly(p-phenylenebenzobisoxazole) Multiphase Nanocomposite *via* Solution Prepolymerization with Superior Microwave Absorption Properties and Thermal Stability, *J. Phys. Chem. C*, 2017, **121**(2), 1072–1081, DOI: **10.1021/acs.jpcc.6b11925**.

204 S. Biswas, G. P. Kar and S. Bose, Tailor-Made Distribution of Nanoparticles in Blend Structure toward Outstanding Electromagnetic Interference Shielding, *ACS Appl. Mater. Interfaces*, 2015, **7**(45), 25448–25463, DOI: **10.1021/acsami.5b08333**.

205 Y. Zhang, T. Pan and Z. Yang, Flexible polyethylene terephthalate/polyaniline composite paper with bending durability and effective electromagnetic shielding performance, *Chem. Eng. J.*, 2020, **389**, 124433.

206 Y. M. Li, C. Deng, Z. Y. Zhao, L. X. Han, P. Lu and Y. Z. Wang, Carbon fiber-based polymer composite *via* ceramization toward excellent electromagnetic interference shielding performance and high temperature resistance, *Composites, Part A*, 2020, **131**, 105769, DOI: **10.1016/j.compositesa.2020.105769**.

207 S. H. Lee, *et al.*, Low percolation 3D Cu and Ag shell network composites for EMI shielding and thermal conduction, *Compos. Sci. Technol.*, 2019, **182**, 107778, DOI: **10.1016/j.compscitech.2019.107778**.

208 A. Gebrekrstos, S. Biswas, A. V. Menon, G. Madras, P. Pötschke and S. Bose, Multi-layered stack consisting of PVDF nanocomposites with flow-induced oriented MWCNT structure can supress electromagnetic radiation, *Composites, Part B*, 2019, **166**, 749–757, DOI: **10.1016/j.compositesb.2019.03.008**.

209 R. Ravindren, S. Mondal, K. Nath and N. C. Das, Investigation of electrical conductivity and electromagnetic interference shielding effectiveness of preferentially distributed conductive filler in highly flexible polymer blends nanocomposites, *Composites, Part A*, 2019, **118**, 75–89, DOI: **10.1016/j.compositesa.2018.12.012**.

210 N. K. Hota, N. Karna, K. A. Dubey, D. K. Tripathy and B. P. Sahoo, Effect of temperature and electron beam irradiation on the dielectric properties and electromagnetic interference shielding effectiveness of ethylene acrylic elastomer/millable polyurethane/SWCNT nanocomposites, *Eur. Polym. J.*, 2019, **112**, 754–765, DOI: **10.1016/j.eurpolymj.2018.10.048**.

211 D. P. Schmitz, *et al.*, Electromagnetic interference shielding effectiveness of ABS carbon-based composites manufactured *via* fused deposition modelling, *Mater. Today Commun.*, 2018, **15**, 70–80, DOI: **10.1016/j.mtcomm.2018.02.034**.

212 K. Chizari, M. Arjmand, Z. Liu, U. Sundararaj and D. Therriault, Three-dimensional printing of highly conductive polymer nanocomposites for EMI shielding applications, *Mater. Today Commun.*, 2017, **11**, 112–118, DOI: **10.1016/j.mtcomm.2017.02.006**.
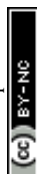
213 K. Zhang, *et al.*, Morphological regulation improved electrical conductivity and electromagnetic interference shielding in poly(l-lactide)/poly(ε-caprolactone)/carbon nanotube nanocomposites *via* constructing stereocomplex crystallites, *J. Mater. Chem. C*, 2017, **5**(11), 2807–2817, DOI: **10.1039/c7tc00389g**.

214 Z. Zeng, C. Wang, Y. Zhang, P. Wang, S. I. Seyed Shahabadi, Y. Pei, M. Chen and X. Lu, Ultralight and highly elastic graphene/lignin-derived carbon nanocomposite aerogels with ultrahigh electromagnetic interference shielding performance, *ACS Appl. Mater. Interfaces*, 2018, **10**(9), 8205–8213, DOI: **10.1021/acsami.7b19427**.

215 C. Wan, Y. Jiao, T. Qiang and J. Li, Cellulose-derived carbon aerogels supported goethite (α-FeOOH) nanoneedles and nanoflowers for electromagnetic interference shielding, *Carbohydr. Polym.*, 2017, **156**, 427–434, DOI: **10.1016/j.carbpol.2016.09.028**.

216 A. D. La Rosa, *et al.*, Recovery of electronic wastes as fillers for electromagnetic shielding in building components: An LCA study, *J. Cleaner Prod.*, 2021, **280**, 124593, DOI: **10.1016/j.jclepro.2020.124593**.

217 M. Rahaman, I. A. Al Ghufais, G. Periyasami and A. Aldalbahi, Recycling and Reusing Polyethylene Waste as Antistatic and Electromagnetic Interference Shielding Materials, *Int. J. Polym. Sci.*, 2020, **2020**, 6421470, DOI: **10.1155/2020/6421470**.

218 A. V. Menon, G. Madras and S. Bose, Mussel-Inspired Self-Healing Polyurethane with 'Flower-like' Magnetic MoS 2 as Efficient Microwave Absorbers, *ACS Appl. Polym. Mater.*, 2019, **1**(9), 2417–2429, DOI: **10.1021/acsapm.9b00538**.

219 A. V. Menon, G. Madras and S. Bose, Ultrafast Self-Healable Interfaces in Polyurethane Nanocomposites Designed Using Diels-Alder 'click' as an Efficient Microwave Absorber, *ACS Omega*, 2018, **3**(1), 1137–1146, DOI: **10.1021/acsomega.7b01845**.

220 A. V. Menon, B. Choudhury, G. Madras and S. Bose, 'Trigger-free' self-healable electromagnetic shielding material assisted by co-doped graphene nanostructures, *Chem. Eng. J.*, 2020, **382**, 122816, DOI: **10.1016/j.cej.2019.122816**.

221 P. Yan, *et al.*, Recyclable, self-healing, absorption-dominated and highly effective electromagnetic shielding elastomers based on bridged micro capacitance structure, *Carbon*, 2020, **166**, 56–63, DOI: **10.1016/j.carbon.2020.04.091**.

222 X. Dai, *et al.*, Recoverable and self-healing electromagnetic wave absorbing nanocomposites, *Compos. Sci. Technol.*, 2019, **174**, 27–32, DOI: **10.1016/j.compscitech.2019.02.018**.

223 S. Li, J. Li, N. Ma, D. Liu and G. Sui, Super-Compression-Resistant Multiwalled Carbon Nanotube/Nickel-Coated Carbonized Loofah Fiber/Polyether Ether Ketone Composite with Excellent Electromagnetic Shielding Performance, *ACS Sustain. Chem. Eng.*, 2019, **7**(16), 13970–13980, DOI: **10.1021/acssuschemeng.9b02447**.

224 H. Fang, *et al.*, Simultaneous improvement of mechanical properties and electromagnetic interference shielding performance in eco-friendly polylactide composites *via* reactive blending and MWCNTs induced morphological optimization, *Composites, Part B*, 2019, **178**, 107452, DOI: **10.1016/j.compositesb.2019.107452**.

225 S. Kashi, R. K. Gupta, T. Baum, N. Kao and S. N. Bhattacharya, Dielectric properties and electromagnetic interference shielding effectiveness of graphene-based biodegradable nanocomposites, *Mater. Des.*, 2016, **109**, 68–78, DOI: **10.1016/j.matdes.2016.07.062**.

226 G. Wang, G. Zhao, S. Wang, L. Zhang and C. B. Park, Injection-molded microcellular PLA/graphite nanocomposites with dramatically enhanced mechanical and electrical properties for ultra-efficient EMI shielding applications, *J. Mater. Chem. C*, 2018, **6**(25), 6847–6859, DOI: **10.1039/c8tc01326h**.

227 G. Wang, *et al.*, Ultralow-Threshold and Lightweight Biodegradable Porous PLA/MWCNT with Segregated Conductive Networks for High-Performance Thermal Insulation and Electromagnetic Interference Shielding Applications, *ACS Appl. Mater. Interfaces*, 2018, **10**(1), 1195–1203, DOI: **10.1021/acsami.7b14111**.

228 S. Kashi, R. K. Gupta, T. Baum, N. Kao and S. N. Bhattacharya, Morphology, electromagnetic properties and electromagnetic interference shielding performance of poly lactide/graphene nanoplatelet nanocomposites, *Mater. Des.*, 2016, **95**, 119–126, DOI: **10.1016/j.matdes.2016.01.086**.

229 T. Kuang, L. Chang, F. Chen, Y. Sheng, D. Fu and X. Peng, Facile preparation of lightweight high-strength biodegradable polymer/multi-walled carbon nanotubes nanocomposite foams for electromagnetic interference shielding, *Carbon*, 2016, **105**, 305–313, DOI: **10.1016/j.carbon.2016.04.052**.

230 D. A. Gopakumar, *et al.*, Cellulose Nanofiber-Based Polyaniline Flexible Papers as Sustainable Microwave Absorbers in the X-Band, *ACS Appl. Mater. Interfaces*, 2018, **10**(23), 20032–20043, DOI: **10.1021/acsami.8b04549**.

231 Z. Wang, *et al.*, Paper-based metasurface: Turning waste-paper into a solution for electromagnetic pollution, *J. Cleaner Prod.*, 2019, **234**, 588–596, DOI: **10.1016/j.jclepro.2019.06.239**.

232 L. Vazhayal, P. Wilson and K. Prabhakaran, Waste to wealth: Lightweight, mechanically strong and conductive carbon aerogels from waste tissue paper for electromagnetic shielding and CO_2 adsorption, *Chem. Eng. J.*, 2020, **381**, 122628, DOI: **10.1016/j.cej.2019.122628**.

233 P. J. Bora, M. Porwal, K. J. Vinoy, Kishore, P. C. Ramamurthy and G. Madras, Industrial waste fly ash cenosphere composites based broad band microwave absorber, *Composites, Part B*, 2018, **134**, 151–163, DOI: **10.1016/j.compositesb.2017.09.062**.

234 P. J. Bora, N. Mallik, P. C. Ramamurthy, Kishore and G. Madras, Poly(vinyl butyral)-polyaniline-magnetically functionalized fly ash cenosphere composite film for electromagnetic interference shielding, *Composites, Part*
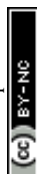
B, 2016, **106**, 224–233, DOI: **10.1016/ j.compositesb.2016.09.035**.

235 P. Lv, *et al.*, Metal-based bacterial cellulose of sandwich nanomaterials for anti-oxidation electromagnetic interference shielding, *Mater. Des.*, 2016, **112**, 374–382, DOI: **10.1016/j.matdes.2016.09.100**.

236 G. George, *et al.*, Green and facile approach to prepare polypropylene/: *In situ* reduced graphene oxide nanocomposites with excellent electromagnetic interference shielding properties, *RSC Adv.*, 2018, **8**(53), 30412–30428, DOI: **10.1039/c8ra05007d**.